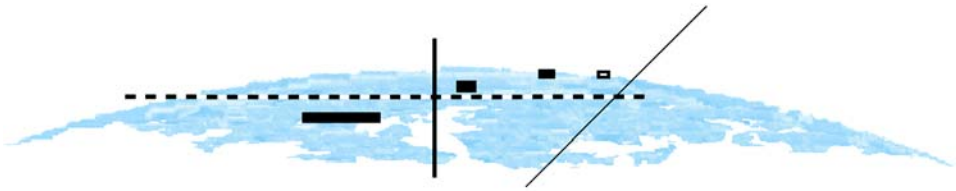

GeoForschungsZentrum Potsdam

STIFTUNG DES ÖFFENTLICHEN RECHTS

Scientific Technical Report

Joachim Höpfner

Parameter variability of the observed polar motions with smaller amplitudes

Paper presented
at the XXVII General Assembly
European Geophysical Society
Nice, France
22-26 April, 2002

Scientific Technical Report STR02/01

Parameter variability of the observed polar motions with smaller amplitudes

Joachim Höpfner

GeoForschungsZentrum Potsdam, Division 1: Kinematics and Dynamics of the Earth,Telegrafenberg, D-14473 Potsdam, Germany; E-mail: ho@gfz-potsdam.de

Abstract. Compared to the Chandler and annual wobbles, the higher-frequency components of polar motion (PM) have substantially smaller amplitudes. Therefore, their study had to wait until higher-quality time series with high temporal resolution, as measured by space geodetic techniques, became available. Based on the combined Earth orientation series SPACE99 computed by the Jet Propulsion Laboratory (JPL) from 1976 to 2000 at daily intervals, we have separated the periodic PM terms by band-pass filtering and found that the persistence of oscillations becomes less with increasing frequency (Höpfner 2001a, b). In order to quantify and better describe the parameter variability of these PM components over time, particularly of eight oscillations with periods ranging between about 650 and 45 days, we computed the radii, direction angles and period lengths from the periodic terms filtered out from the time series. The results clearly show the characteristics and time evolution of the periodic PM components that are important for geophysical interpretations.

Key words: Polar motion, periodic components, parameter (radii, directions, period lenghts), variability

1 Introduction

Variations in the Earth's rotation relative to the terrestrial body-fixed reference frame are measured by polar motion (PM) and changes in the length-of-day (LOD).The theoretical foundations for such phenomena, especially PM, were derived between the mid-18th to mid-19th centuries (Euler, 1758; Lagrange, 1788; Poinsot, 1834; Peters, 1844). In order to confirm the existence of the PM of the Earth in terms of latitudinal variations, intensive efforts were undertaken at several observatories towards the end of the 19th century. This was finally achieved by Küstner (1888) in observations carried out between 1884 and 1885 at the Berlin Observatory. Chandler (1891, 1892) determined that the periodic latitude variations are comprised of two superposed components with periods of ca. 365 and 427 days. Activities quickly intensified, led by the Central European Arc Measurement (i.e., the forerunner of the International Association of Geodesy, IAG), which after considerable effort led to the establishment in 1899 of the International Latitude Service (ILS) as the first permanent worldwide scientific cooperation, with a central bureau and six observing sites. The ILS stations were all located along the northern parallel of $39^o08'$ and were well-distributed in longitude and equipped with visual zenith telescopes (VZTs). The sites were Mizusawa (Japan), Tschardjui (Russia), Carloforte (Italy), Gaithersburg (USA), Cincinnati (USA) and Ukiah (USA). The task of the ILS was to make latitude observations (Helmert and Albrecht, 1899) in order to monitore the motion of the Earth's pole of rotation. In 1962, since the PM was derived from both latitude and longitude variations, the ILS was renamed the International Polar Motion Service (IPMS). Since the middle of the 1970s, precise space geodesy techniques such as VLBI (Very Long Baseline radio Interferometry), LLR (Lunar Laser Ranging), SLR (Satellite Laser Ranging) were used, while from 1992 GPS (Global Positioning System) and DORIS (Doppler Orbit determination and Radiopositioning Integrated on Satellite) have come into use. In 1988, the IPMS was discontinued with the commencement of the International Earth Rotation Service (IERS) (see, e.g., Höpfner (2000)).

These efforts mean that polar motion data is available from the mid-19th century to the present. For the period 1846-1890, the PM solutions derived by Rikhlova (see Fedorov et al. 1972) is based on three series of absolute declination observations at Pulkovo, Greenwich, and Washington. From about 1890-1900, there were astronomical latitude observations at 20 independent stations. Over the next 80 years, the ILS and later the IPMS provided systematic and continuous latitude observations at the ILS stations. Other latitude measurements were made with different types of instruments (astrolabes, photographic zenith tubes and visual zenith telescopes) at independent stations on the Northern and Southern

hemispheres, in particular from 1955 when the Bureau International de l'Heure (BIH), hosted by the Paris Observatory (and operating from 1919), installed its own polar motion service denoted as Service International Rapide des Latitudes (SIR), and more intensivly from 1957 at the beginning the International Geophysical Year (IGY). Based on the measurements of the Earth orientation parameters by optical astrometry, there are a number of PM solutions in terms of ILS and non-ILS time series. A review of these PM time series can be found in Höpfner (2000) and the references therein. Compared to the earlier PM data, the combined Earth orientation series based on the precise space-geodetic measurements has a higher accuracy and a higher temporal resolution. For more information on the historical and scientific problems of polar motion, see Dick, McCarthy and Luzum (2000).

Recent studies dealt with the substantially smaller PM components are made by Höpfner (1995, 1996), Kosek et al. (1995, 1997) and Kołaczek et al. (2000). Using the combined Earth orientation series SPACE99, as computed by the Jet Propulsion Laboratory (JPL) from 1976 to 2000 with one-day sampling (Gross, 2000), we have studied the dominant components of PM, including the low-frequency component (the secular drift of the Earth's pole) and the Chandler and annual wobbles, focusing on quantifying their temporal variability (Höpfner, 2001a). The remaining motions, after removing the major terms from the PM coordinates of the time series SPACE99, were analysed with respect to the polar motions with smaller amplitudes (Höpfner, 2001b). In this study, we continue our previous PM investigations, the objective being to quantify and better describe the parameter variability of substantially smaller PM components over time.

2 Fundamentals

If a 2-D geophysical process *x(t)* with the time variable *t* is given by the real functions $x_1(t)$ and $x_2(t)$, its equation may be written in complex notation as

$$x(t) = x_1(t) \; + \; i \;\; x_2(t) \; . \tag{1}$$

Using the polar coordinate system for the following discussion, the radii (amplitudes) *r(t)* and direction angles $\gamma(t)$ of the process *x(t)* are obtained by

$$r(t) = |x(t)| = |x_1(t) \; + \; i \;\; x_2(t)| = \left(x_1(t)^2 + x_2(t)^2\right)^{\frac{1}{2}} \tag{2}$$

and

$$\gamma(t) = \arctan \frac{x_2(t)}{x_1(t)} \; . \tag{3}$$

In our case, the 2-D geophysical process is the PM that has temporal periods ranging from a few hours to many years. According to equation (1), the periodic components $x_f(t)$ with a frequency f of the PM have the form

$$x_f(t) = x_{1,f}(t) \; + \; i \;\; x_{2,f}(t) \; . \tag{4}$$

For each component $x_f(t)$, according to formulas (2) and (3), the radii (amplitudes) $r_f(t)$ and direction angles $\gamma_f(t)$ are expressed as

$$r_f(t) = |x_f(t)| = |x_{1,f}(t) \; + \; i \;\; x_{2,f}(t)| = \left(x_{1,f}(t)^2 + x_{2,f}(t)^2\right)^{\frac{1}{2}} \tag{5}$$

and

$$\gamma_f(t) = \arctan \frac{x_{2,f}(t)}{x_{1,f}(t)} \; . \tag{6}$$

Concerning an elliptic motion, the maxima of the radii (amplitudes) $r_f(t)$ are the semi-major axes *a* at the times t_a and the minima the semi-minor axes *b* at the times t_b,

$$a = r_f(t_a) = max\{r_f(t)\} \quad \text{and} \quad b = r_f(t_b) = min\{r_f(t)\} \; , \tag{7}$$

while the pertinent direction angles $\gamma_f(t)$ are their directions γ_a and γ_b,

$$\gamma_a = \gamma_f(t_a) \quad \text{and} \quad \gamma_b = \gamma_f(t_b). \tag{8}$$

The period lengths *T* of an elliptic motion are obtained from the differences between the times t, if the direction angles $\gamma_f(t)$ are 0^o and 360^o, and from the double differences between the times t_a of the semi-major axes *a* (maxima) and t_b

Table 1. Time intervals of the periodic components of polar motion with smaller amplitudes filtered out from the combined Earth orientation series SPACE99 (JPL) given in MJD and calendar days

Component	Time interval (MJD)	Time interval (calendar days)
Quasi-biennial	45861.0 ... 48933.0	1983/12/13 ... 1992/11/07
300-day	47056.0 ... 47558.0	1987/09/18 ... 1989/02/01
Semi-Chandler	44466.0 ... 50148.0	1980/08/15 ... 1996/03/06
Semi-annual	44397.0 ... 50217.0	1980/06/07 ... 1996/05/14
4-month	44728.0 ... 49886.0	1981/05/04 ... 1995/06/18
90-day	46641.0 ... 47937.0	1986/07/30 ... 1990/03/23
2-month	44859.0 ... 49755.0	1981/09/12 ... 1995/02/07
1.5-month	44827.0 ... 49787.0	1981/08/11 ... 1995/03/11

of the semi-minor axes *b* (minima).

The numerical eccentricity ϵ used as a dimensionless measure for the ellipticity of a periodic motion is computed according to the formula

$$\epsilon = \frac{(a^2 - b^2)^{\frac{1}{2}}}{a}. \tag{9}$$

If $\epsilon = 0$, then there is a circular motion; if $0 < \epsilon < 1$, then there is an elliptic motion. The closer ϵ is to 0, the more circular is its motion; while the closer ϵ is to 1, the more elliptic is its motion.

Note that equations (4) to (9) are the basis of the following considerations, where estimations for the components of polar motion are of the elliptic type.

3 Data processing and results

In this study, we use the periodic PM terms separated by band-pass filtering from the combined Earth orientation series SPACE99 after removing the low-frequency, Chandler and annual terms; see Höpfner (2001a, b). In particular, the filtered components are the following eight polar motions that exhibit smaller amplitudes: The quasi-biennial wobble, the 300-day wobble, the semi-Chandler wobble, the semi-annual wobble, the 4-month wobble, the 90-day wobble, the 2-month wobble and the 1.5-month wobble. For these polar motions, $x_f(t)$ are given by the x_1- and x_2-coordinates at one-day intervals according to equation (4) where the x_1-axis points towards the Greenwich Meridian and the x_2-axis towards the 90^o E longitude. For the time intervals of the periodic PM components, see Table 1.

The data processing for each motion $x_f(t)$ includes the following two steps:
(1) Calculating the radii $r_f(t)$ according to equation (5) and their direction angles $\gamma_f(t)$ according to equation (6).
(2) Determining the semi-major axes *a* and semi-minor axes *b* as the maxima and minima of the radii according to equation (7), their directions γ_a and γ_b according to equation (8) and the period lengths *T* as the time differences at the direction angles of 0^o and 360^o and as the double time differences at the semi-major axes *a* and at the semi-minor axes *b*.

Variations in the parameters of the periodic components of polar motion over time are presented in Figs 1 to 4 (divided as Fig. 1 for the quasi-biennial wobble (upper part) and 300-day wobble (lower part), Fig. 2 for the semi-Chandler wobble (upper part) and semi-annual wobble (lower part), Fig. 3 for the 4-month wobble (upper part) and 90-day wobble (lower part) and Fig. 4 for the 2-month wobble (upper part) and 1.5-month wobble (lower part)).

Especially for each elliptic motion $x_f(t)$, we find displayed
(a) the radius variation at the top, with the superior envelope indicating the change in the semi-major axis and the inferior envelope the change in the semi-minor axis,
(b) the direction courses of the radii at the centre, with distinctive markers indicating the direction angles of the semi-major and semi-minor axes, and
(c) the period variation at the bottom.

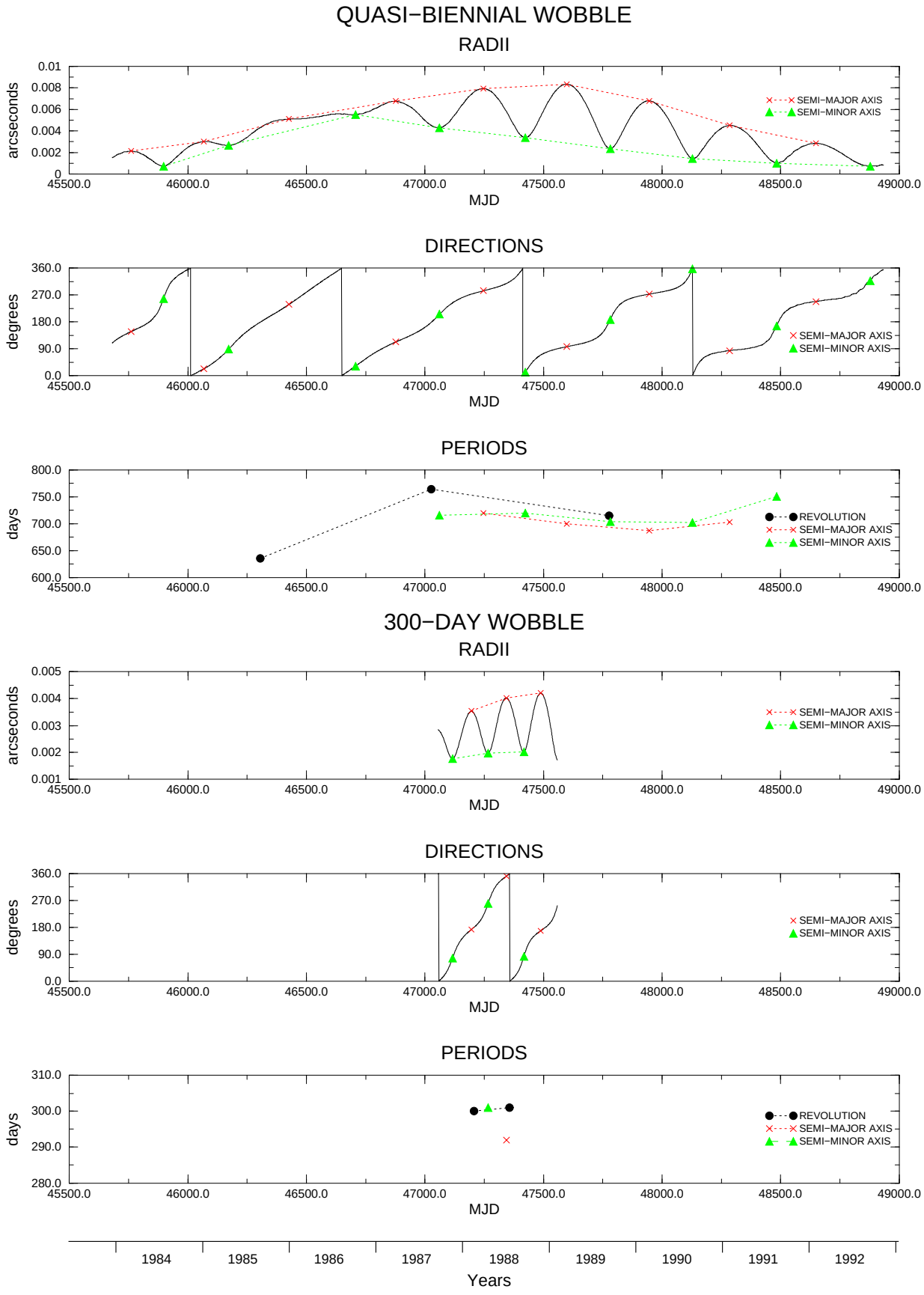

Figure 1. Variations in the parameters of the periodic components of polar motion: Quasi-biennial wobble (upper part) and 300-day wobble (lower part). In each part, the curves shown are: Radii, semi-major and semi-minor axes (top), directions of the radii (centre) and periods (bottom)

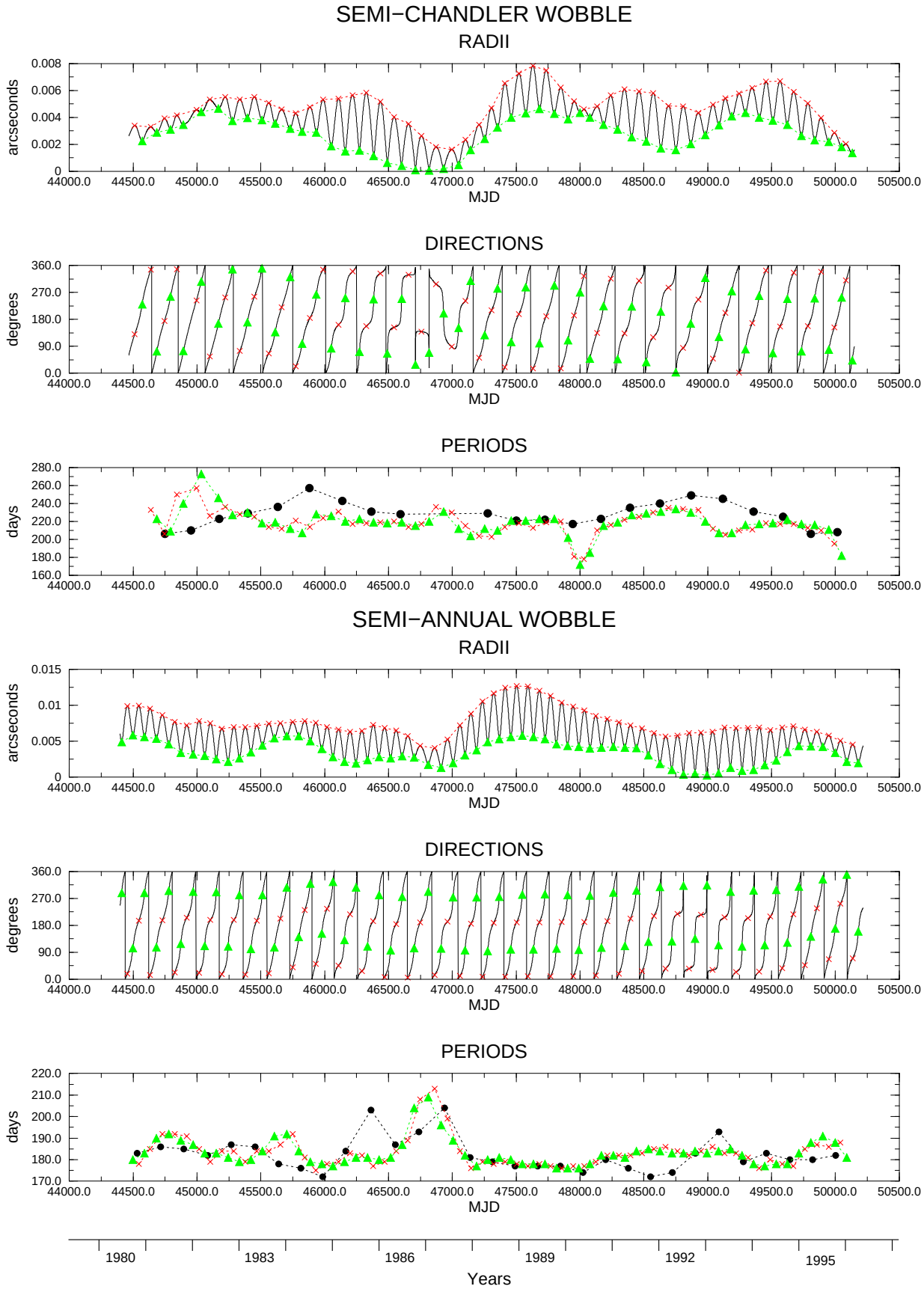

Figure 2. Variations in the parameters of the periodic components of polar motion: Semi-Chandler wobble (upper part) and semi-annual wobble (lower part). In each part, the curves shown are: Radii, semi-major and semi-minor axes (top), directions of the radii (centre) and periods (bottom). The markers used here are the same as in Fig. 1

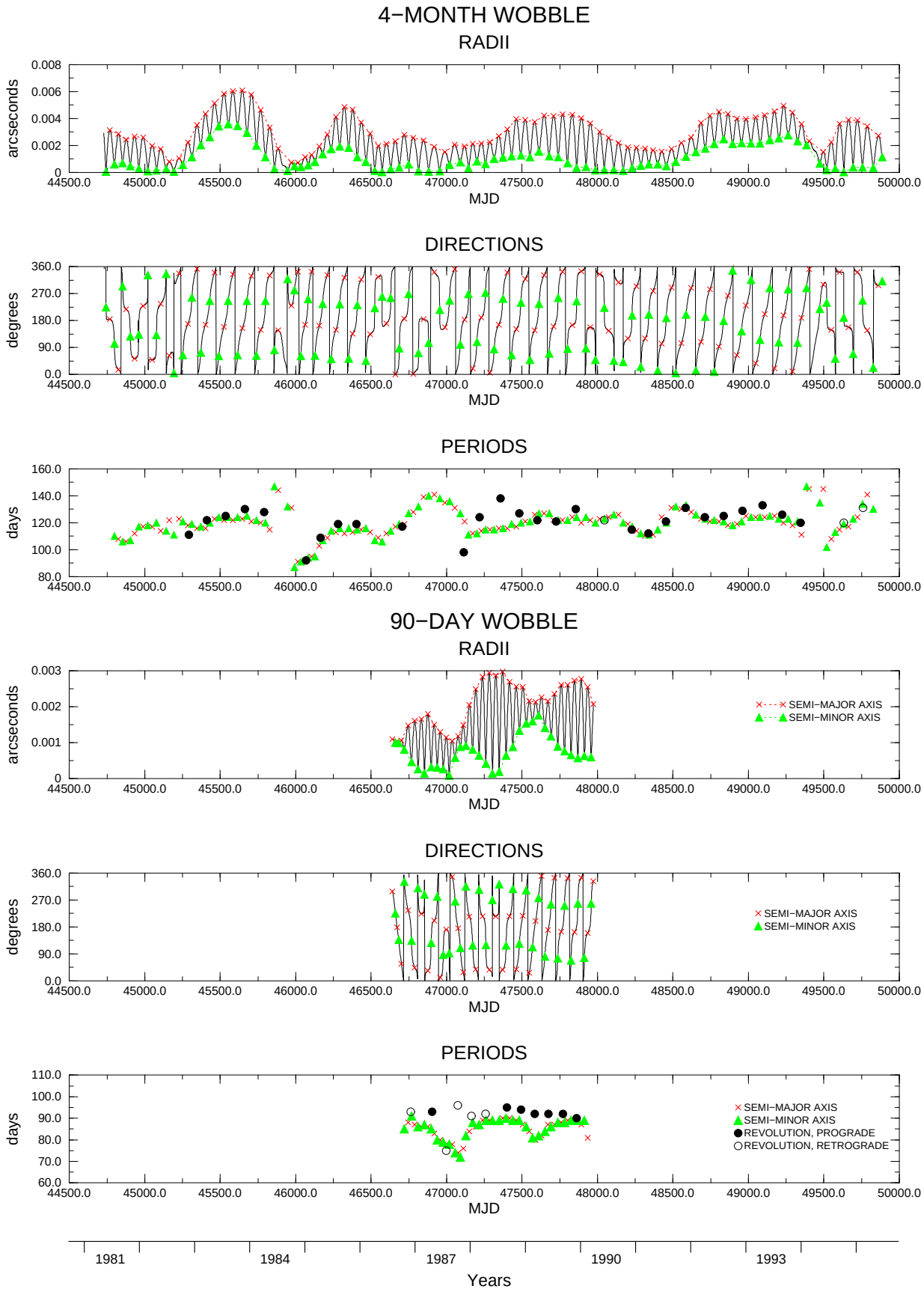

Figure 3. Variations in the parameters of the periodic components of polar motion: 4-month wobble (upper part) and 90-day wobble (lower part). In each part, the curves shown are: Radii, semi-major and semi-minor axes (top), directions of the radii (centre) and periods (bottom)

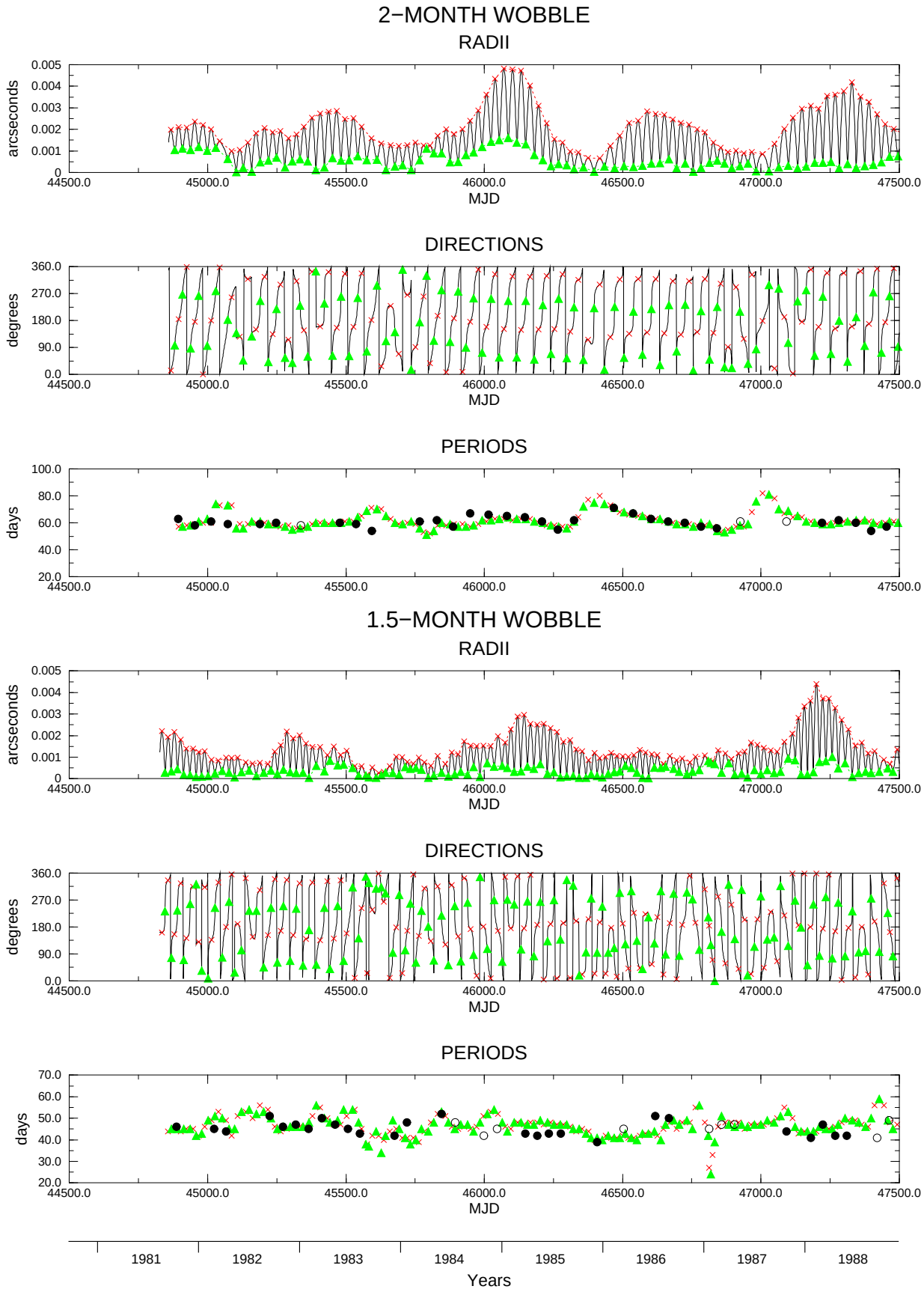

Figure 4. Variations in the parameters of the periodic components of polar motion: 2-month wobble (upper part) and 1.5-month wobble (lower part). In each part, the curves shown are: Radii, semi-major and semi-minor axes (top), directions of the radii (centre) and periods (bottom)

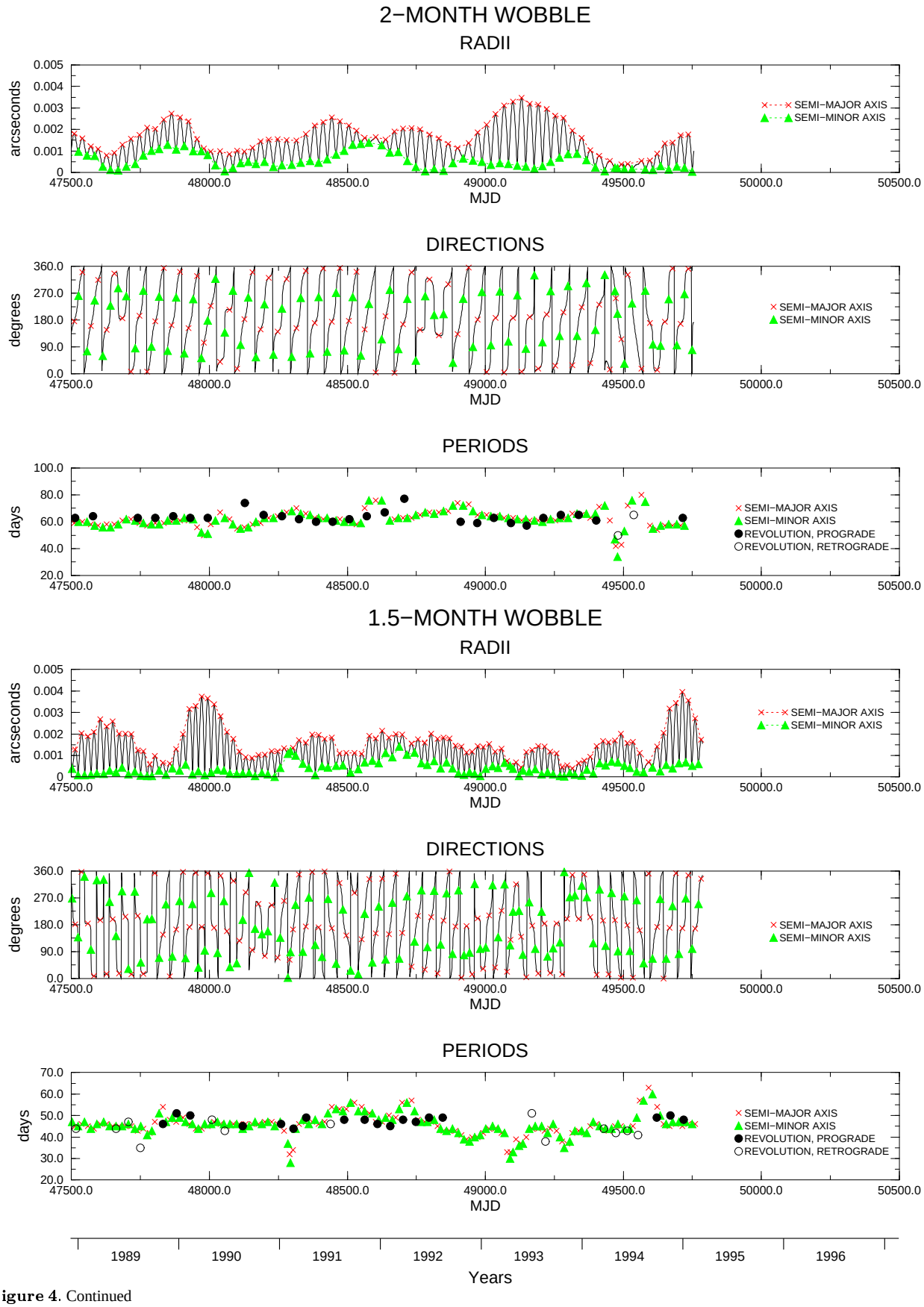

Figure 4. Continued

Table 2. Characteristics of the periodic components of polar motion with smaller amplitudes filtered out from the combined Earth orientation series SPACE99 (JPL)

Component	Period (days)	Motion direction	Type	Numerical eccentricity	Semi-major axis (mas)	Direction of the semi-major axis	Semi-minor axis (mas)
Quasi-biennial	625 ... 750	prograde	variably elliptic	0.47 ... 0.98	2.1 ... 8.4	from 148^0 to 84^0	0.7 ... 5.6
300-day	290 ... 300	prograde	clearly elliptic	0.83 ... 0.88	3.5 ... 4.2	ca. 170^0	1.7 ... 2.0
Semi-Chandler	200 ... 240	prograde	oval to elliptic	0.49 ... 0.99	1.6 ... 7.8	systemat. variable	0.1 ... 4.7
Semi-annual	170 ... 200	prograde	elliptic	0.64 ... 0.99	4.1 ... 12.7	from 6^0 to 70^0	0.3 ... 5.8
4-month	110 ... 130	mostly prograde	elliptic	0.76 ... 0.99	0.8 ... 6.1	ca. 150^0, later shifted	0.1 ... 3.6
90-day	75 ... 95	progr.; retrogr.	oval to elliptic	0.24 ... 0.99	1.0 ... 3.0	from 60^0 to 330^0	0.1 ... 1.7
2-month	55 ... 70	mostly prograde	clearly elliptic	0.47 ... 0.99	0.2 ... 4.8	from 135^0 to 225^0	0.1 ... 1.6
1.5-month	40 ... 55	progr.; retrogr.	clearly elliptic	0.55 ... 0.99	0.4 ... 4.4	from 135^0 to 200^0	0.1 ... 1.4

Concerning the results plotted in Figs. 1 to 4, it should be noted that:
- The smaller the difference between the semi-major and semi-minor axes, the more circular is the periodic component of polar motion; while the larger the difference, the more elliptic is the periodic component.
- If the direction angle increases, then the motion is prograde, i.e. counter-clockwise; if it decreases, then the motion is retrograde, i.e. clockwise.
- Each direction course of 0^o to 360^o (or vice versa of 360^o to 0^o) indicates an elapsed prograde (retrograde) revolution of the PM component of interest, with its turning-points indicating the extreme sites (maxima and minima of the radii) of the component.
- The more straight the direction course over an revolution, the more circular is the periodic motion. Conversely, the more curved the direction course, the more elliptic is the motion.

In order to show the variability in the orientation and the ellipticity of the periodic PM components, the revolution motions over their analysis intervals are presented in the Appendix (Figures A1 to A7). The relevant characteristics of the components, in particular the period length, motion direction, type of motion, numerical eccentricity, semi-major axis and its direction angle and semi-minor axis, are summmarized in Table 2.

4 Discussion of the results

In general, the results presented in Figs 1 to 4 show very well the parameter variability of the smaller PM components relative to the JPL system. As previously stated in Höpfner (2001b), the persistence of the elliptic motions becomes less with higher frequencies. We shall now discuss and assess separately the results for the different wobbles.

Quasi-biennial wobble (Fig. 1, upper part; Fig. A1, upper part)
During 1984-1992, there was a varying elliptic prograde motion with a period ranging between 625 and 750 days. See about 4.5 revolutions with considerable variability in radius. Particularly obvious is the semi-major axis, where there was an increase from 2.1 to 8.4 mas at 1988/1989 and then a decrease to 2.9 mas. Note that the revolution from 46012.0 to 46648.0 (in MJD), i.e. from Nov. 1984 to Aug. 1986, is elapsed as a circular spiral (see Fig. A1, upper part, and in particular the second picture). After this, the ellipticity becomes larger. Regarding the orientation of the elliptic motion related to the semi-major axis, we find a systematic change in its direction of 148^0 to 84^0 over four revolutions, i.e. by -16^0 per revolution.

300-day wobble (Fig. 1, lower part; Fig. A1, lower part)
This component is seen as an elliptic prograde motion over about two cycles in 1987/1988. The elliptic motion has a semi-major axis of ca. 4 mas at a direction of ca. 170^0 and a semi-minor axis of ca. 2 mas. Its period length varies between 290 and 300 days.

Semi-Chandler wobble (Fig. 2, upper part; Fig. A2)
For the period 1980-1996, we computed 25 cycles of the semi-Chandler wobble. As can be seen, it exists as a prograde motion varying in its ellipticity of oval over elliptic to high elliptic, while also being very small in magnitude (see Fig. A2, in particular the 11th picture), and again oval to elliptic. For example, the cycle with the largest semi-major axis of 7.8 mas at a direction of about $11^0$and a semi-minor axis of 4.3 mas (plotted in the 14th picture of Fig. A2) is elapsed over 221 days from 47613.0 to 47834.0 (in MJD), i.e. from Apr. to Nov. 1989, while the smallest motion took place over 452 days (or two cycles) from 46710.0 to 47162.0, i.e. from Oct. 1986 to Dec. 1987 (plotted in the 11th picture of

Fig. A2). In Fig. 3, upper part, see the top panel for the variation in radius of 0.1 to 7.8 mas and the middle panel for the pertinent direction angles. The two other maxima of the radius cited in Höpfner (2001b) refer to the cycles over 229 days from 46251.0 to 46480.0 and over 233 days from 49476.0 to 49699.0 (plotted in the 9th and 22nd pictures of Fig. A2). For the orientation of the elliptic motion, note that there is an average direction shift of -24^0 per cycle. As can be seen in the bottom panel of Fig. 3 (upper part), the period length varies between 200 and 240 days over time, except at 45000.0 and 48000.0 (in MJD), i.e. Feb. 1982 and May 1990, when it is about 260 and 180 days, respectively.

Semi-annual wobble (Fig. 2, lower part; Fig. A3)
The semi-anual wobble separated over 32 cycles in 1980-1996 is found as an elliptic prograde motion with a semi-major axis varying between 4.1 and 12.7 mas and a semi-minor axis varying between 0.3 and 5.8 mas, where the orientation of motion is relatively stationary. In particular, the direction of the semi-major axis lies between 6^0 and 70^0. We obtained the semi-annual cycle with the largest semi-major axis of 12.7 mas at a direction angle of about 8^0 elapsed over 176 days from 47404.0 to 47580.0 (in MJD), i.e. Sept. 1988 to March 1989 (plotted in the 18th picture of Fig. A3). The four cycles (25) to (28) of Fig. A3 with period lengths of 173, 182, 193 and 178 days have the smallest semi-minor axes and therefore the biggest ellipticity (ϵ = 0.99). They are been from Jan. 1992 to Jan. 1994. By contrast, the 177-day cycle elapsed from 45548.0 to 45725.0, i.e. Aug. 1983 to Jan. 1984 (plotted in the 8th picture), is evident by an oval motion (ϵ = 0.64). The period ranges from 170 to 200 days, except in 1986/1987 (from 46600.0 to 47000.0), when it reaches about 210 days.

4-month wobble (Fig. 3, upper part; Fig. A4)
The 4-month wobble is numerically available over 39 revolutions in 1981-1995. It is obtained as an elliptic primarily prograde motion with considerable variability both in radius and ellipticity. Obviously, if the radius becames very small, then there are some cases of retrogade motion over certain time intervals, such as from 44728.0 to 44934.0, from 47950.0 to 48156.0 and from 49509.0 to 49829.0 (plotted in the pictures (1)+(2), (26) and (37)-(40) of Fig. A4). We find the following four cycles with the largest motions from 45473.0 to 45597.0 (May to Sept 1983), 46224.0 to 46342.0 (June to Oct. 1985), 47668.0 to 47788.0 (May to Sept. 1989) and 49161.0 to 49287.0 (June to Oct. 1993) (plotted in the pictures (7), (13), (24) and (35) of Fig. A4). Note that the maximum semi-major axes reach over 4.1 to 6.1 mas and that the main orientation of the elliptic motion lies at about 150^0 from 45250.0 to 48000.0, while afterwards there is a systematic shift of about -12^0 per cycle over the further time. The period varies between 110 and 130 days with two exceptations where it was 150 days in 1984 and 1994.

90-day wobble (Fig. 3, lower part; Fig. A5)
For this wobble, the results computed and shown over the period 1986-1990 relate to 16 cycles. We can see that the elliptic motion is alternately retrograde and prograde over time intervals of different length. The radius varies between 0.1 and 3.0 mas and the ellipticity varies between oval to elliptic. It should be noted that the 91-day cycle from 47212.0 to 47303.0 (Feb. to May 1988) is elapsed retrogradly and the 95-day cycle from 47350.0 to 47445.0 (June to Oct. 1988) progradly, both with a maximum semi-major axis of about 3.0 mas at a direction of about 37^0 (plotted in the pictures (8) and (10) of Fig. A5). Over the analysis period, the orientation of the elliptic motion relative to the semi-major axis varies from about 60^0 to 330^0 and the period between 85 and 95 days, except that it is only about 75 days in 1987 (near 47000.0) when the semi-minor axis is also very small.

2-month wobble (Fig. 4, upper part; Fig. A6)
The 2-month wobble obtained over about 80 cycles between 1981-1995 is a variable elliptic with primarily a prograde motion. Concerning the extremes in its time evolution, we notice the following cycles - with maximum semi-major axes from 44925.0 to 44982.0 (Nov. 1981 to Jan. 1982; 44953.0: semi-major axis of 2.4 mas at a direction of about 177^0), from 45367.0 to 45446.0 (Feb. to Apr. 1983; 45437.0: 2.8 mas at 343^0), from 46049.0 to 46113.0 (Dec. 1984 to Feb. 1985; 46071.0: 4.8 mas at 152^0), from 46571.0 to 46633.0 (May to July 1986; 46588.0: 2.8 mas at 141^0), from 47312.0 to 47371.0 (June to July 1988; 47329.0: 4.1 mas at 161^0), from 47836.0 to 47899.0 (Nov. 1989 to Jan 1990; 47863.0: 2.7 mas at 161^0) and from 49122.0 to 49178.0 (May to July 191993; 49131.0: 3.5 mas at 7^0) (plotted in the pictures (2), (10), (21), (29), (41), (50) and (69) of Fig. A6) and - with minimum radii from 45103.0 to 45158.0 (May to July 1982; radius is < 1.5 mas), from 46356.0 to 46432.0 (Oct. to Dec. 1985; < 0.8 mas), from 47031.0 to 47060.0 (Aug. to Sept. 1987; < 1.4 mas), from 47610.0 to 47709.0 (March to June 1989; < 1.4 mas), from 48026.0 to 48090.0 (May to July 1990; < 1.1 mas) and from 49433.0 to 49506.0 (March to May 1994; < 0.6 mas) (plotted in pictures (5), (26), (36), (46), (53) and (74) of Fig. A6). The orientation of the elliptic motion relative to the semi-major axis lies between 135^0 and 225^0. If the radii are rather small, then the motion is also elapsed retrogradly over these time intervals. Such examples can be found in the pictures (5), (8)-(10), (15), (35)-(38), (64) and (75)+(76) of A6. The period length of the wobble varies between 55 and 70 days with three exceptations, in particular in 1987 (near 47000.0), 1991/1992 (near 48600.0) and 1994 (near 49500.0) when there are only small radii.

Table 3. Estimated uncertainty of a daily value for the x_1- and x_2-components of polar motion of the combined Earth orientation series EOP (IERS) C04 and SPACE99 (JPL)

Period	EOP (IERS) C04 (mas)	SPACE99 (JPL) (mas)
1962 ... 1967	30	
1968 ... 1971	20	
1972 ... 1979	15	2.5
1980 ... 1983	2	0.8
1984 ... 1995	0.7	0.3
1996 ... 1999	0.2	0.1

1.5-month wobble (Fig. 4, lower part; Fig. A7)
The 1.5-month wobble analysis includes about 100 cycles between 1981-1995. This component varies with an elliptic motion of alternately prograde and retrograde direction. The biggest motion cycles can be found in Fig. A7: (1), (11), (27), (46), (55), (62) and (97). Their semi-major axes and directions are: 2.2 mas at 161^0 (44835.0), 2.0 mas at 326^0 (45332.0), 3.0 mas at 176^0 (46144.0), 4.4 mas at 358^0 (47200.0), 2.7 mas at 196^0 (47604.0), 3.3 mas at 355^0 (47950.0) and 4.0 mas at 169^0 (49714.0). Over a large number of cycles, the semi-major axis has the magnitude of only about 1.2 mas. For the orientation of the elliptic motion, we find that the direction of the semi-major axis varies between 135^0 and 200^0 during most of the examined time interval. Concerning some retrograde cycles with clear ellipticity, e.g., pictures (25), (38)-(41), (56)-(58) and (91)-(93) of Fig, A7, they are seen to have semi-major axes of 1.0 to 2.6 mas. In general, the period length lies between 40 and 55 days, except in 1987 (near 46800.0), 1991 (near 48300.0), 1993 (near 49100.0) and 1994 (49600.0) when the radii are considerably smaller and do not show much variability.

Concerning the quality of our results, we can only give a general assessment. Our study is based on the combined Earth orientation series SPACE99 developed by JPL. Also, since 1962, the combined daily Earth orientation series EOP(IERS)C04 as computed by IERS is available (IERS, 2000). Therefore, both time series should be compared. For this purpose, a summary of the estimated uncertainty of a daily value for the x_1- and x_2-components is given in Table 3. For the time series EOP (IERS) C04, the uncertainty improves by replacing the classical method for measuring polar motion by space-geodetic techniques over the periods examined. By contrast, the precision of the SPACE99 series (beginning in 1976) is better since only space-geodetic techniques are used. Concerning the differences between the combined Earth orientation series SPACE99 and EOP(IERS)C04, the root-mean-square (rms) obtained is 2.930 mas from 1976 to 1999, but only 0.222 mas from 1987 to 1999 for the x_1-component, and 2.671 mas from 1976 to 1999 and 0.201 mas from 1987 to 1999 for the x_2-component. Prior to 1984, there is greater variability in the differences, particularly in the x_1-component. The reason for this is that the different approaches used by JPL and IERS to correct the bias and rate of the individual series before they are combined (Gross, 2000). Therefore, we believe that the JPL series used in this study is more accurate than the IERS series. Hence, based on the space-geodetic techniques with milliarcsecond accuracy, our results for smaller PM components do not appear to have a significant noise over their time intervals, therefore are realistic.

Using a least-square fit, the parameters and associated uncertainties of the Chandler and annual wobbles of polar motion are computed from the filtered terms for the x_1- and x_2-components in their temporal variability in the JPL system (Höpfner, 2001a). The standard deviations obtained are very small, between ± 0.02 and ± 0.09 mas for the semi-axes and ± 0.63 and ± 1.93 degrees for the direction angles of the Chander wobble, and between ± 0.01 and ± 0.12 mas for the semi-axes and ± 0.08 and ± 0.71 degrees for the direction angles of the annual wobble. Considerating these uncertainties, we find that the precision level of our results for the PM components of interest is about an order of magnitude smaller. To compare our results with previous work (see Introduction), we find similar results as previously presented (Höpfner, 2001b). While there is generally agreement between the results, some differences exist if the motions are substantially small. Since the comparison estimates are referred to the IERS system, small discrepancies may be due to systematic differences between the IERS and JPL systems.

5 Concluding remark

Our study is based on the periodic polar motions in the polar coordinate system. Relative to the JPL system, the results derived from the filtered PM terms in the Cartesian coordinate system are radii, direction angles and period lengths. The curves clearly exhibit the characteristics and time evolution of the various PM components that are important for geophysical studies. Here, the largest motion is the semi-annual wobble showing a maximum semi-major axis of up to 13 mas, followed by the quasi-biennial and semi-Chandler wobbles with maximum semi-major axes up to 8 mas, the 4-month wobble with a maximum semi-major axis up to 6 mas and the 2-month wobble up to 5 mas. Moreover, the 300-day and 1.5-month wobbles have maximum semi-major axes of up to 4 mas, while the 90-day wobble has a maximum major axis up to 3 mas. Finally, it should be noted that the polar motions with period lengths of 4 months and less are elapsed not only progradly, but also retrogradly.

Changes in atmospheric angular momentum (AAM) are the dominant cause of PM (and variations of Earth rotation, measured by changes in the length of day (LOD),) on interannual, seasonal and intraseasonal time scales. Therefore, the AAM time series could be processed in a similar manner as done for the combined Earth orientation series SPACE99 so that the atmospheric excitation portions related to PM may be further considered.

Acknowledgement. Thanks to Kevin Fleming for his linguistic advice that helped to improve the quality of this paper.

Appendix

Figures A1 to A7 show the time evolutions of the periodic PM components over the analysis intervals in terms of the revolution motions in consecutive pictures. Here, a full cycle is plotted in each picture, if so elapsed. Note that, in each picture, the date given in MJD is the start of the curve and the arrow indicates the direction of the motion. For the date of the end of the curve, see the subsequent picture. In Fig. A1, the quasi-biennial wobble is plotted in five pictures in the upper part and the 300-day wobble in two pictures in the lower part. Figure A2 shows the semi-Chandler wobble in 25 pictures and Fig. A3 the semi-annual wobble in 33 pictures. See Fig. A4 for the 4-month wobble shown in 40 pictures, Fig. A5 for the 90-day wobble in 16 pictures, Fig. A6 for the 2-month wobble in 79 pictures and Fig. A7 for the 1.5-month wobble in 98 pictures.

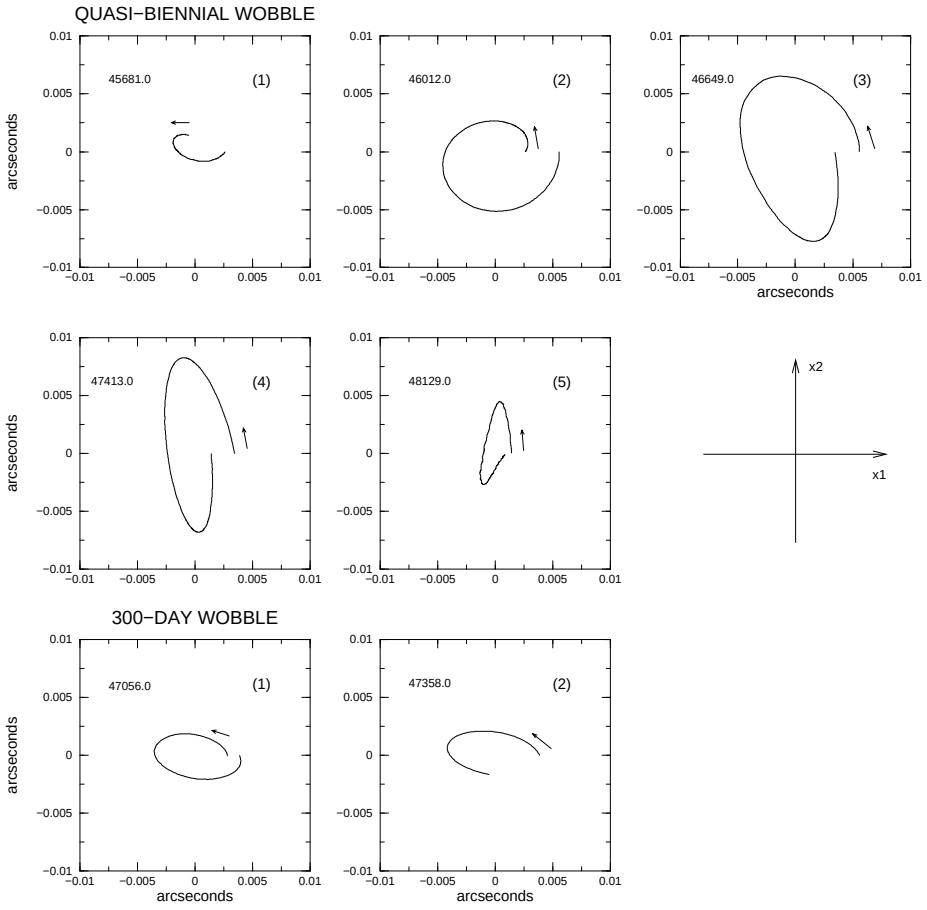

Figure A1. Quasi-biennial wobble (upper part) and 300-day wobble (lower part). In each part, the curves shown are the revolution motions over the analysis interval (from left to right and from top to bottom). The x_1-axis points towards the Greenwich meridian, and the x_2-axis towards 90^oE longitude. For the revolution times in years, see Fig. 1

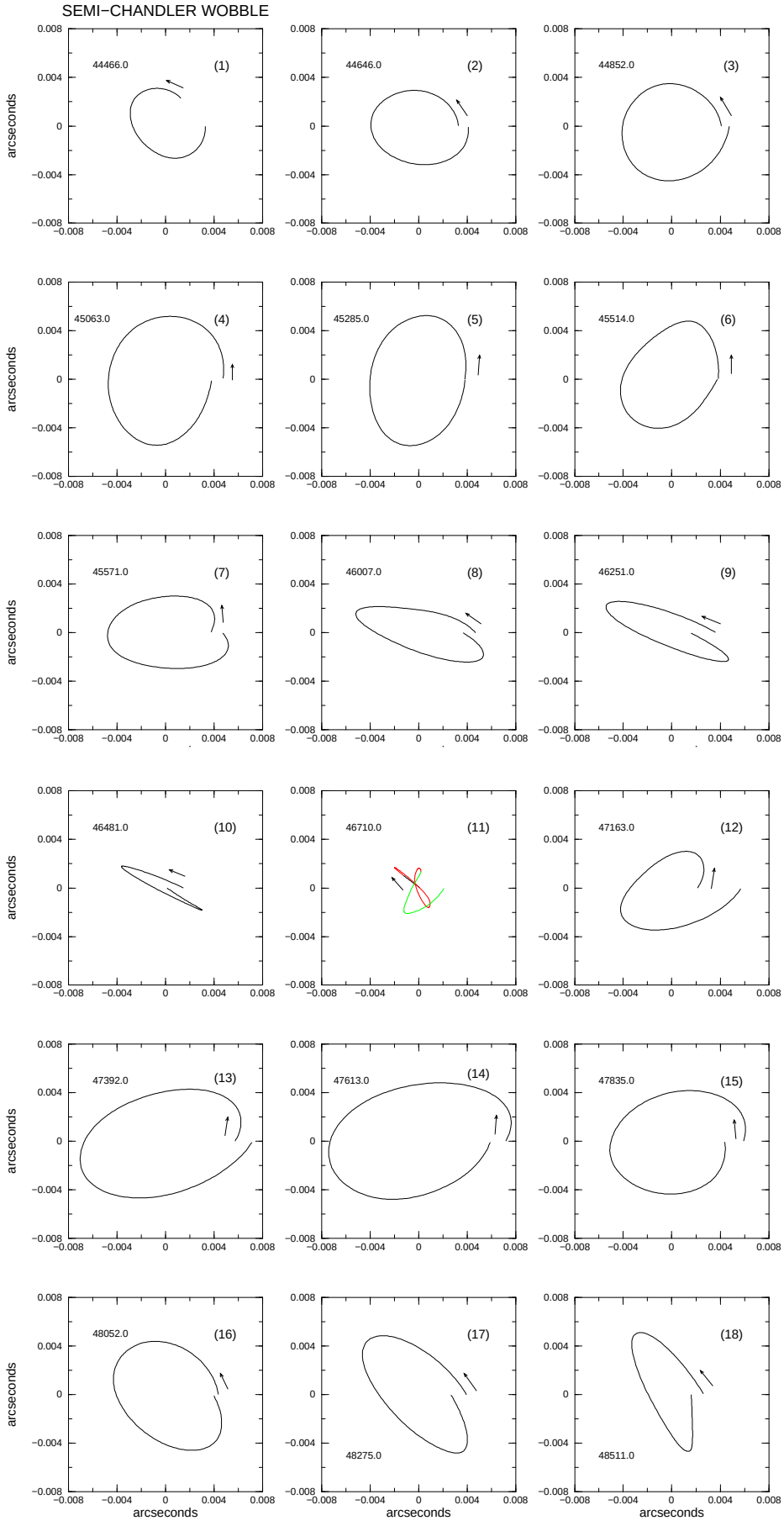

Figure A2. Semi-Chandler wobble. The curves shown are the revolution motions over the analysis interval (from left to right and from top to bottom). The x_1-axis points towards the Greenwich meridian, and the x_2-axis towards 90^oE longitude. For the revolution times in years, see Fig. 2

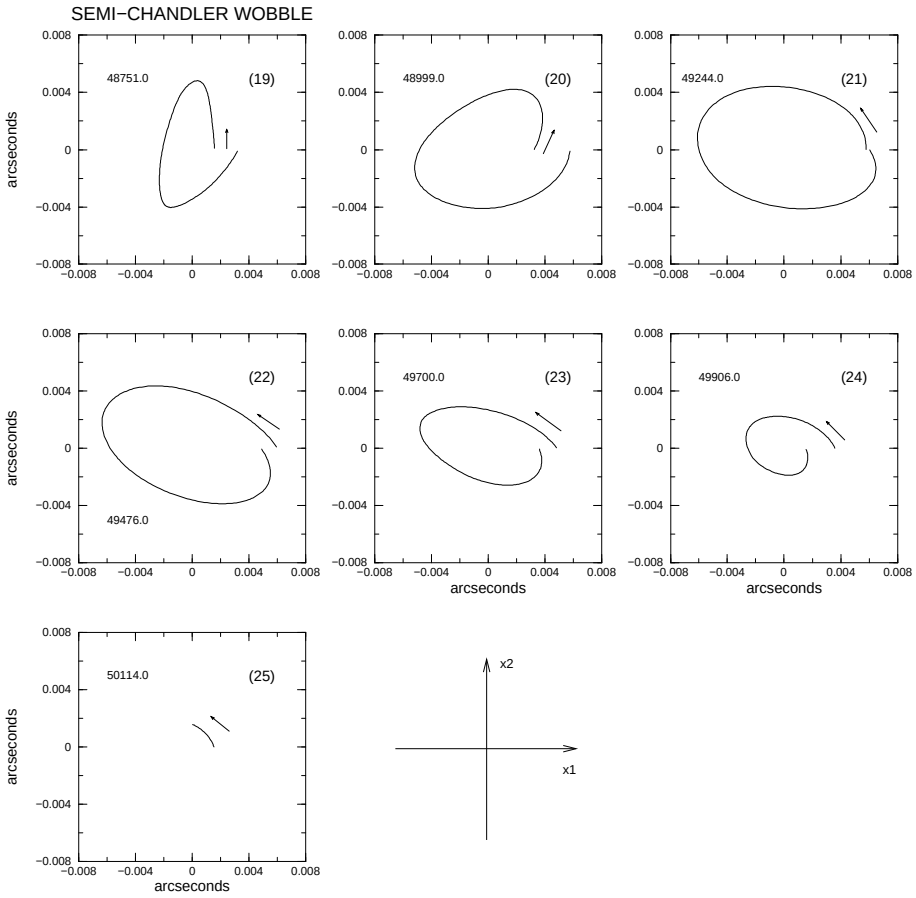

Figure A2. Continued

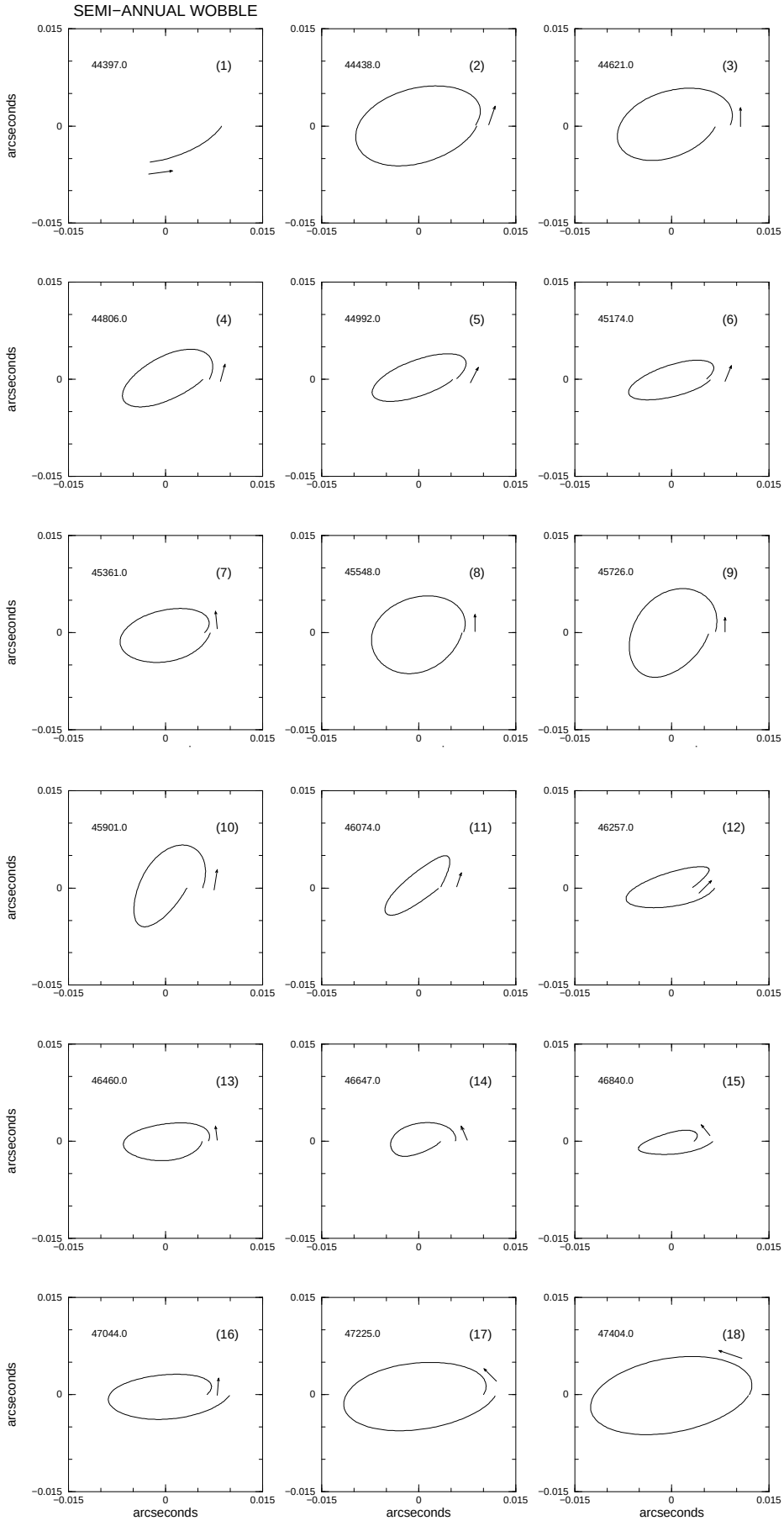

Figure A3. Semi-annual wobble. The curves shown are the revolution motions over the analysis interval (from left to right and from top to bottom). The x_1-axis points towards the Greenwich meridian, and the x_2-axis towards 90^oE longitude. For the revolution times in years, see Fig. 2

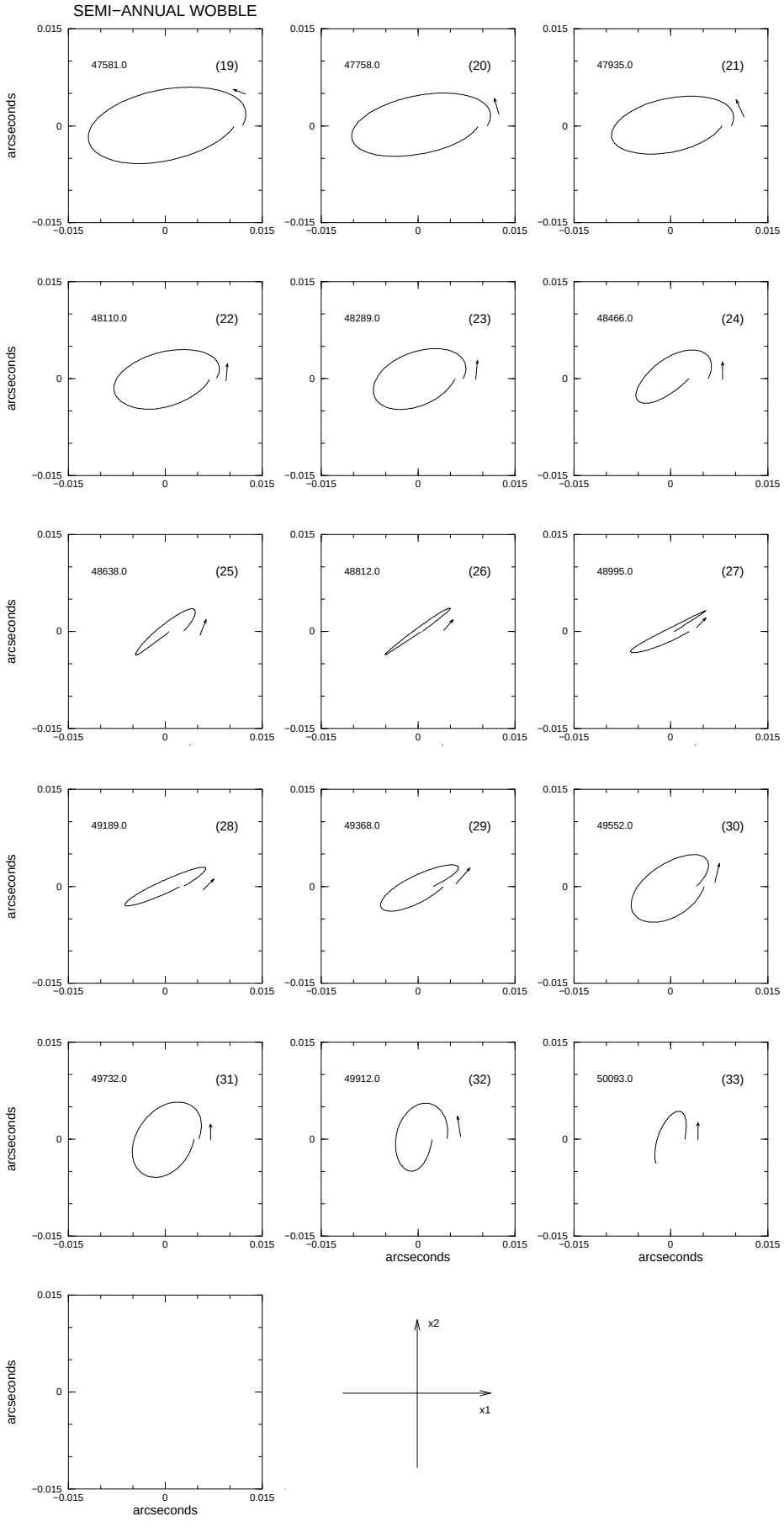

Figure A3. Continued

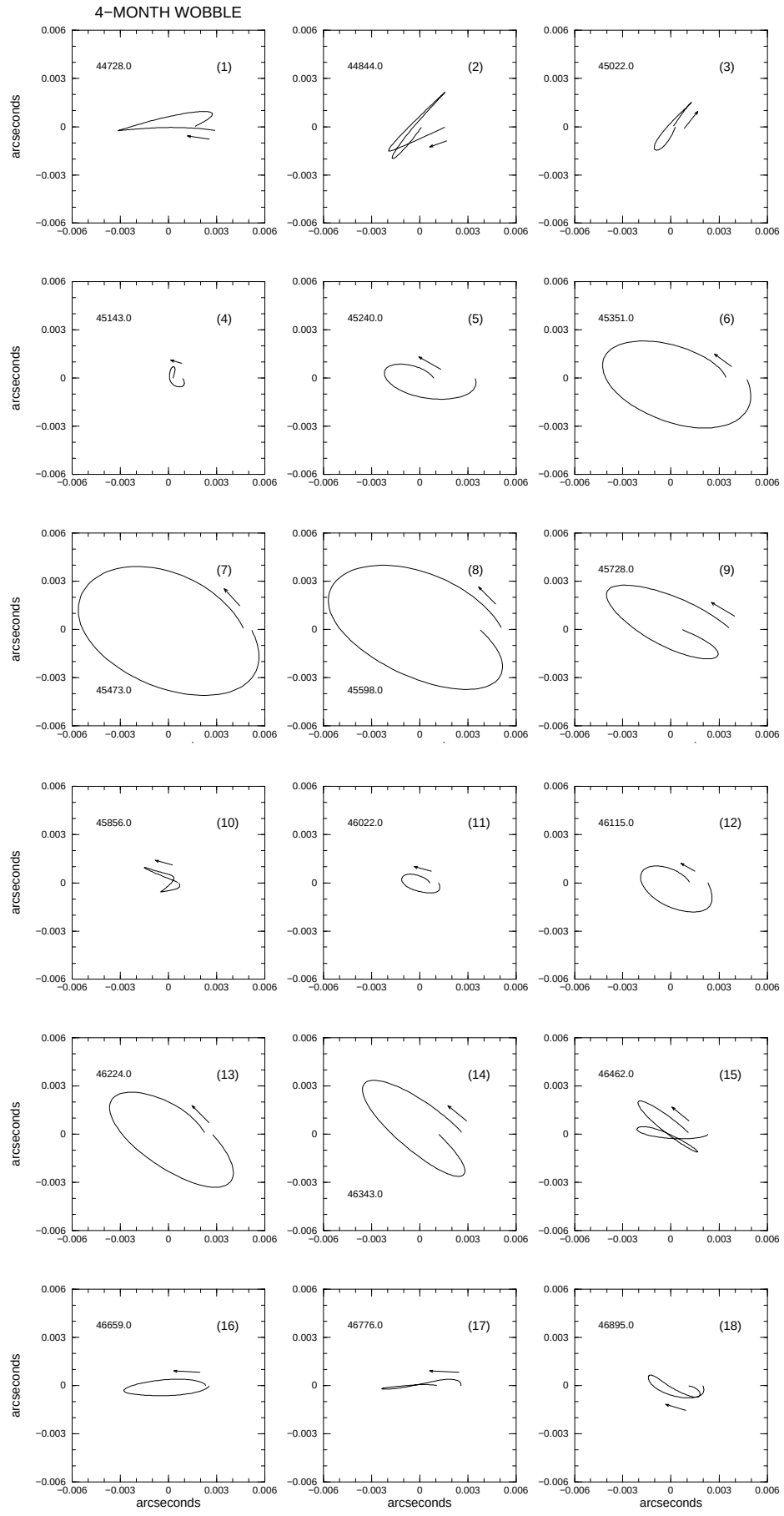

Figure A4. 4-month wobble. The curves shown are the revolution motions over the analysis interval (from left to right and from top to bottom). The x_1-axis points towards the Greenwich meridian, and the x_2-axis towards 90^oE longitude. For the revolution times in years, see Fig. 3

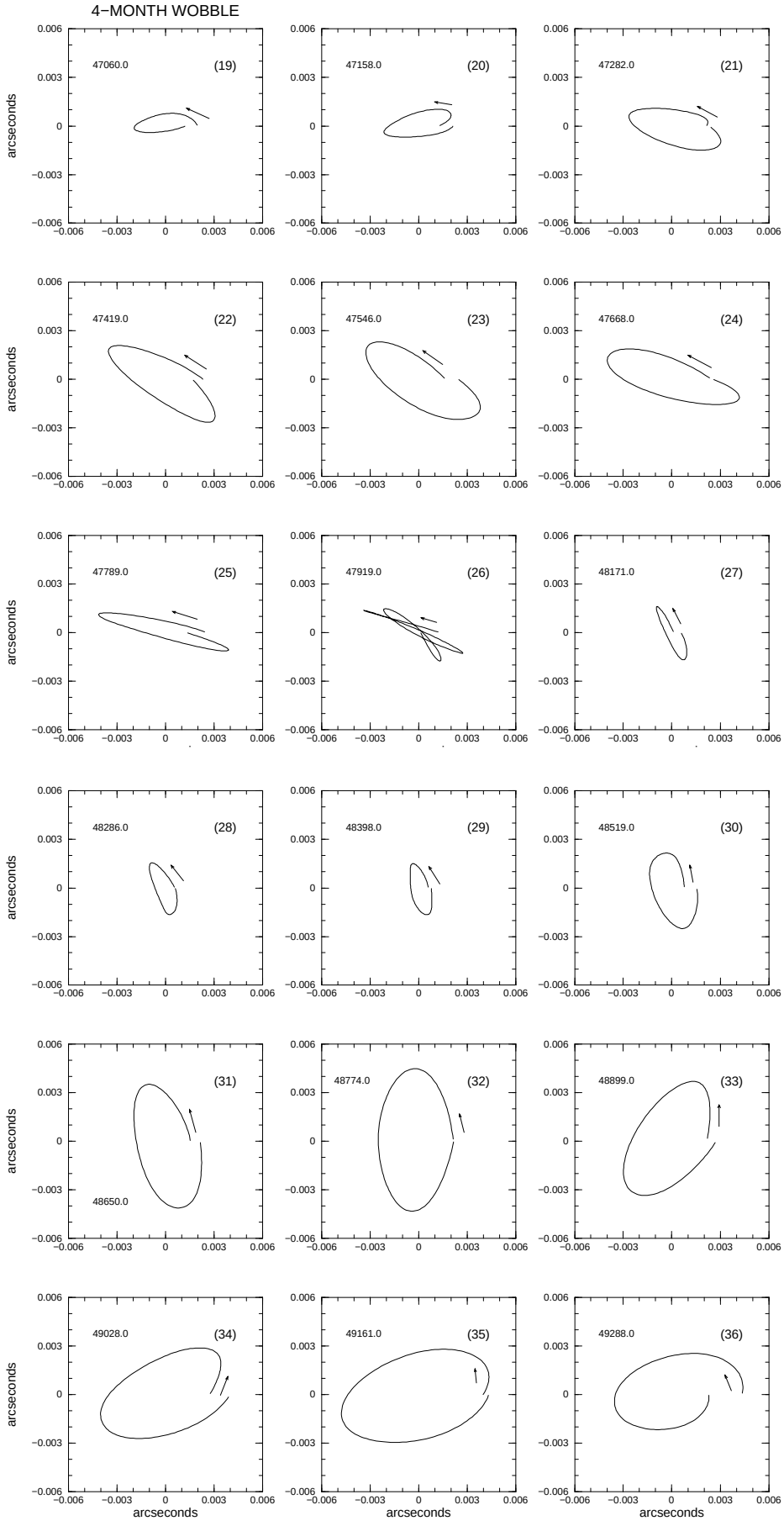

Figure A4. Continued

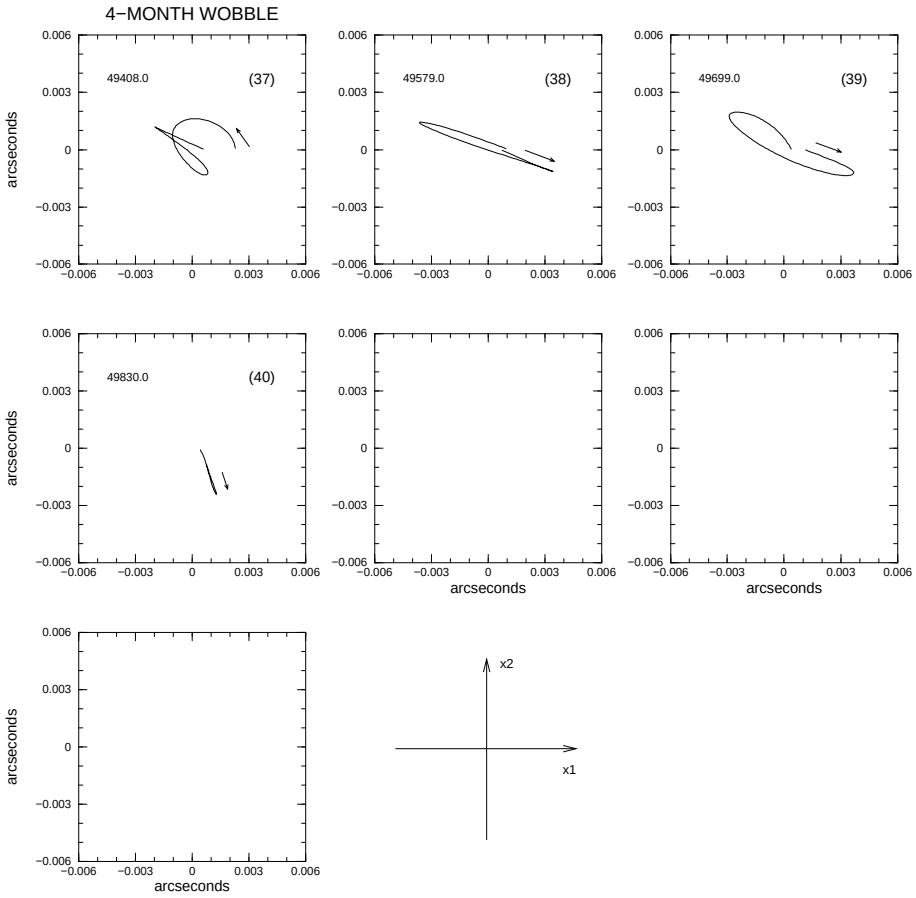

Figure A4. Continued

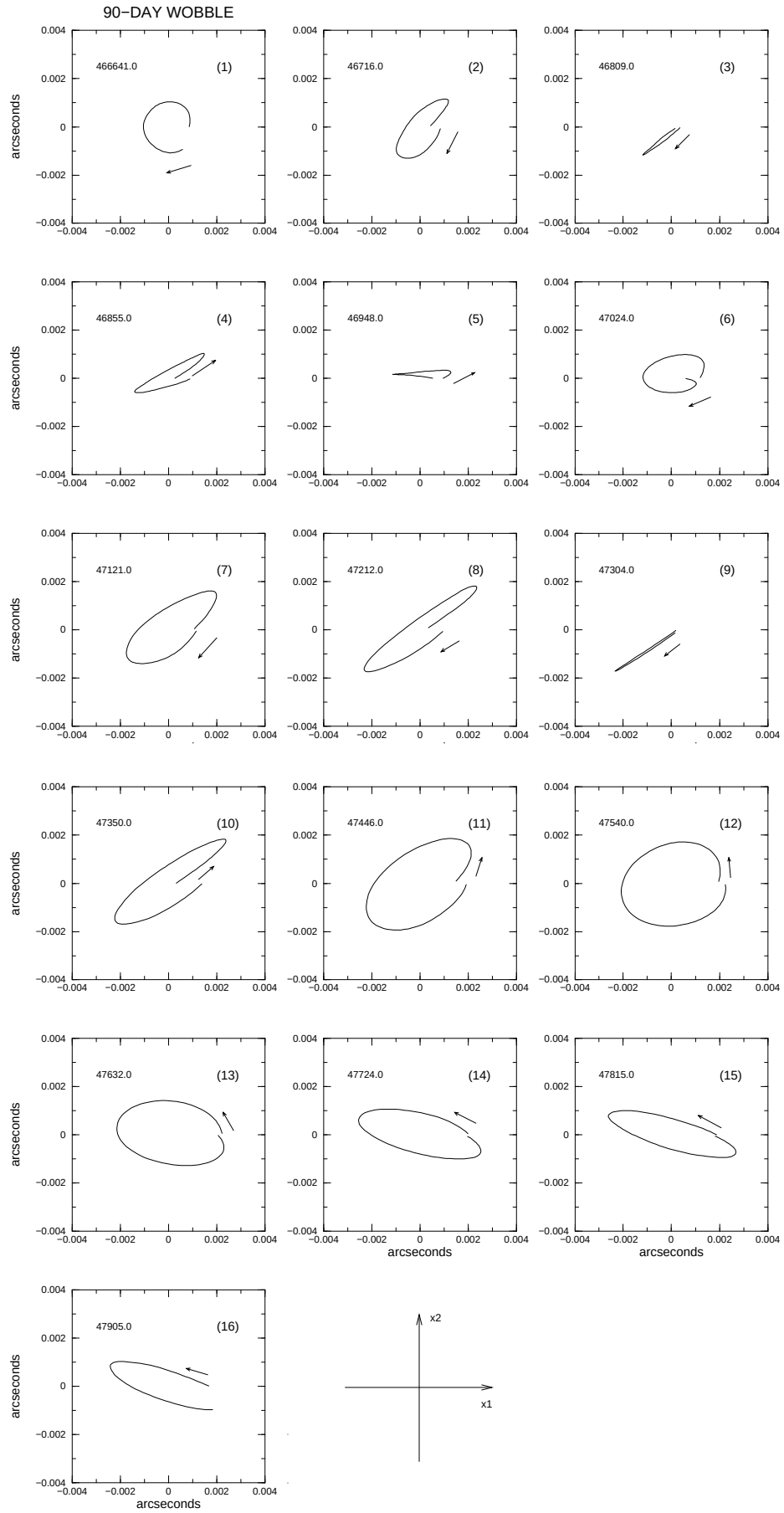

Figure A5. 90-day wobble. The curves shown are the revolution motions over the analysis interval (from left to right and from top to bottom). The x_1-axis points towards the Greenwich meridian, and the x_2-axis towards 90^oE longitude. For the revolution times in years, see Fig. 3

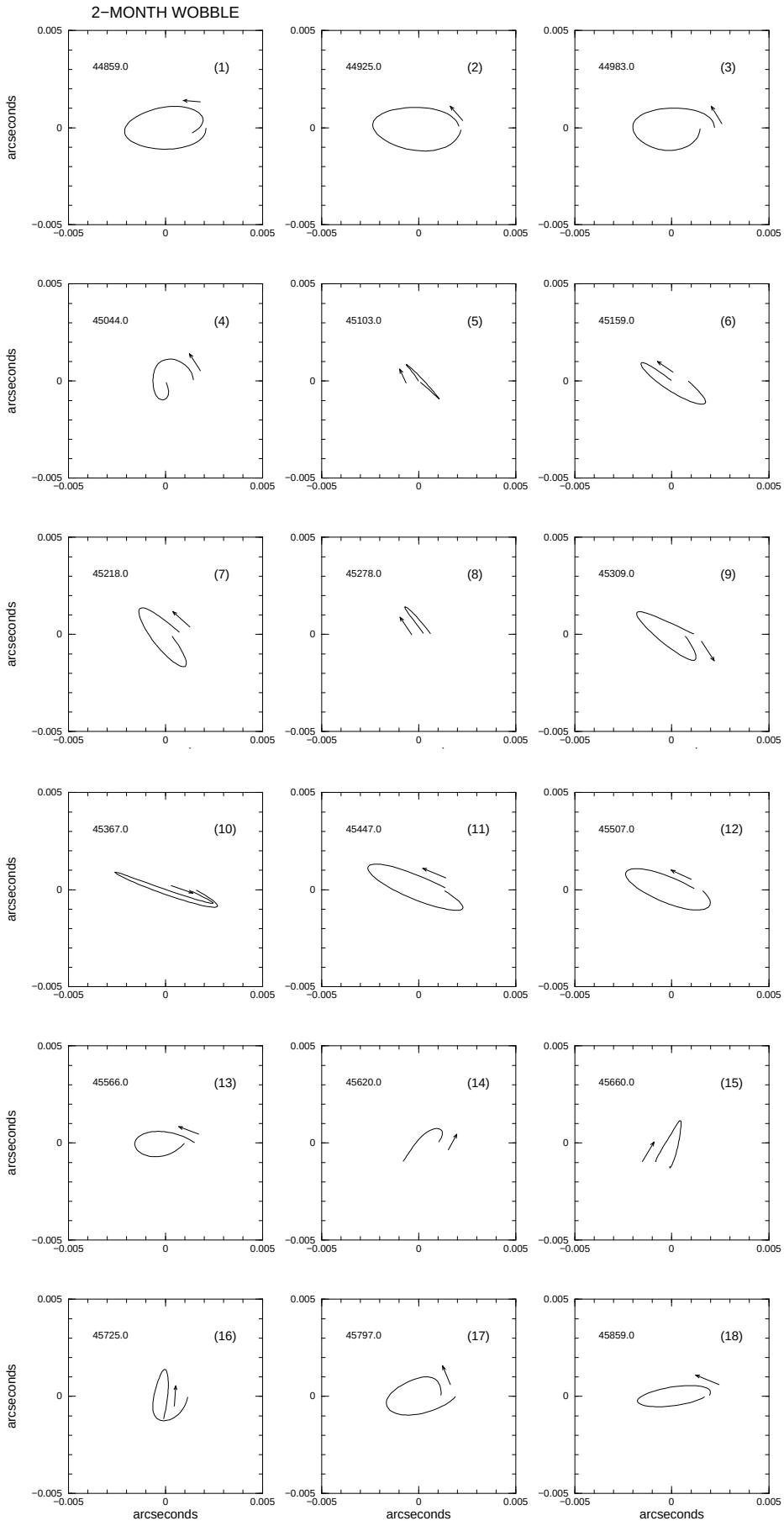

Figure A6. 2-month wobble. The curves shown are the revolution motions over the analysis interval (from left to right and from top to bottom). The x_1-axis points towards the Greenwich meridian, and the x_2-axis towards 90^oE longitude. For the revolution times in years, see Fig. 4

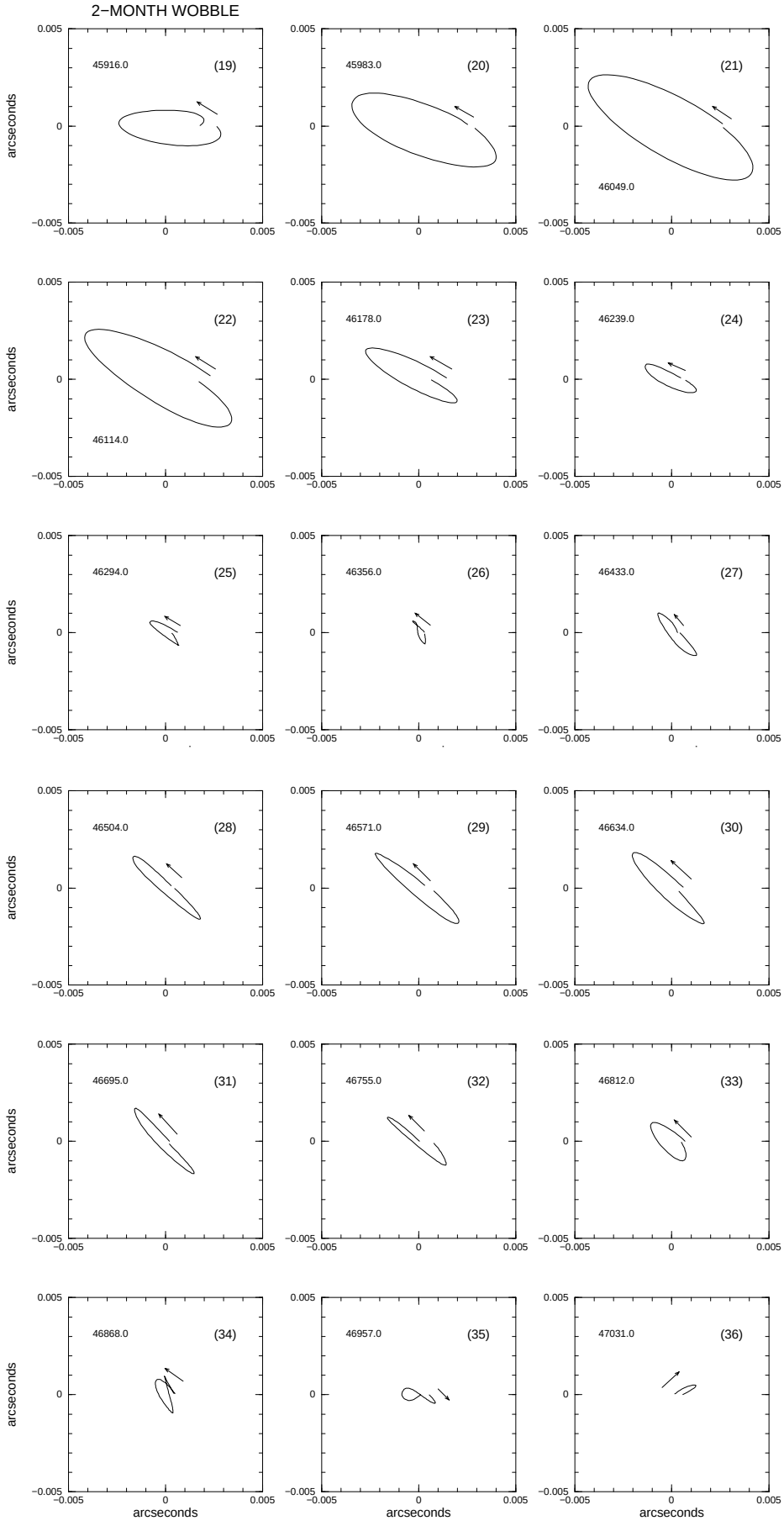

Figure A6. Continued

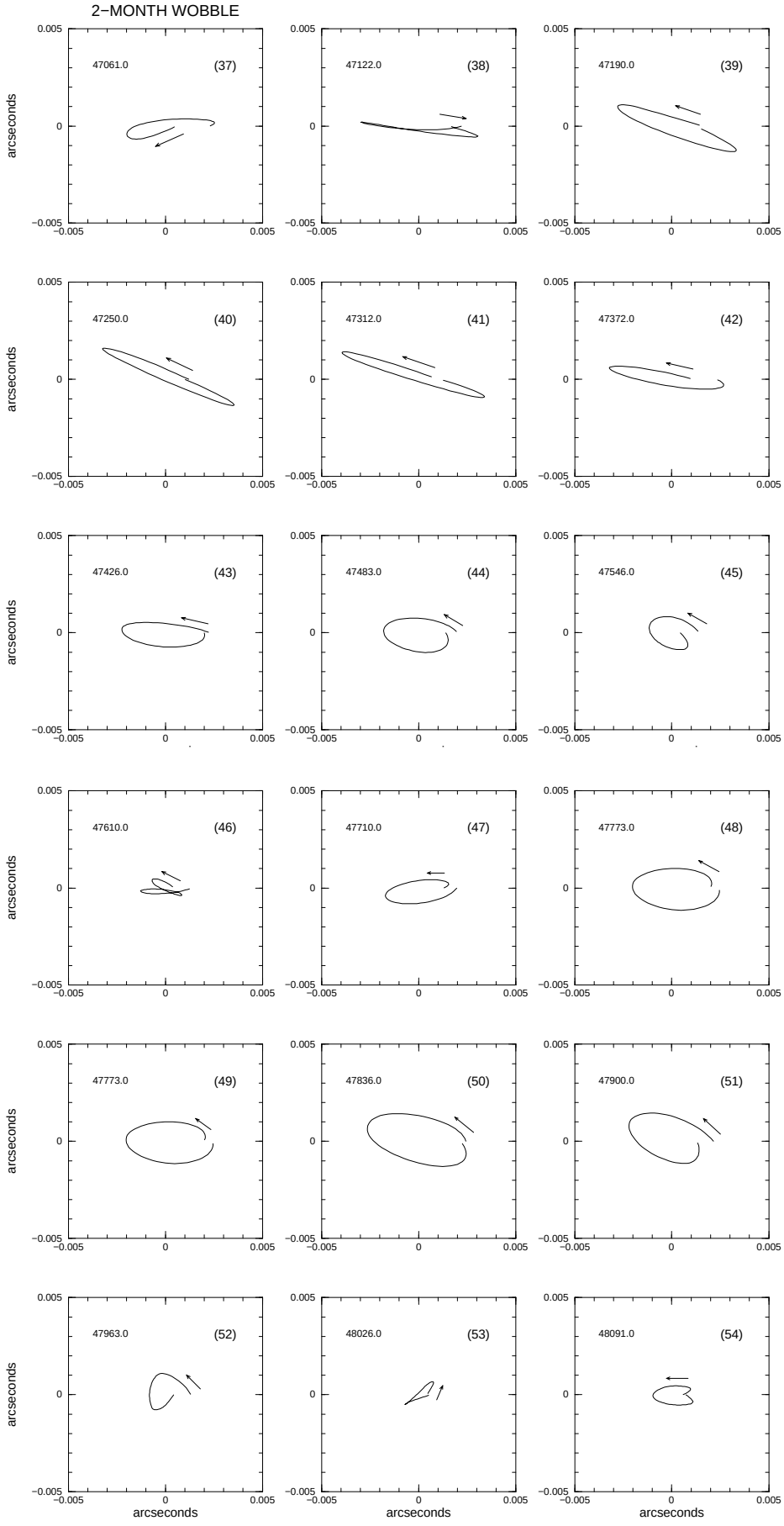

Figure A6. Continued

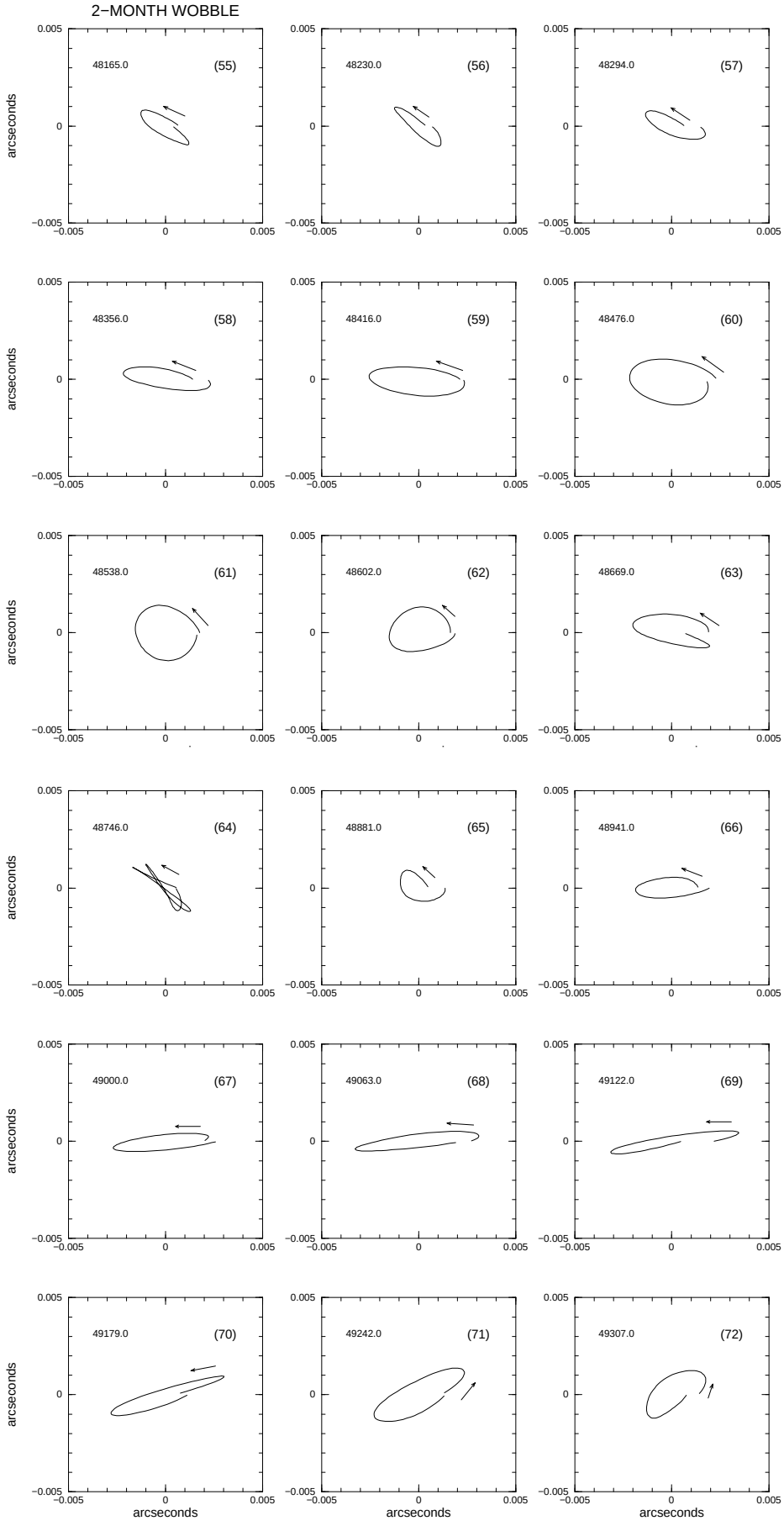

Figure A6. Continued

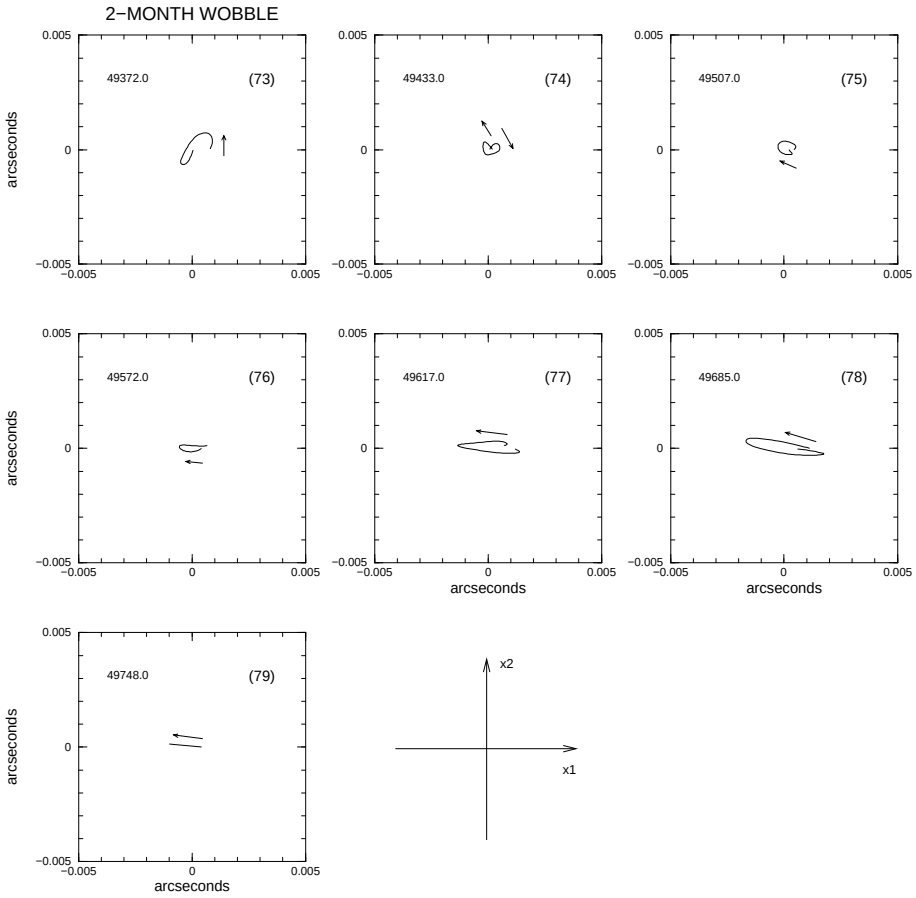

Figure A6. Continued

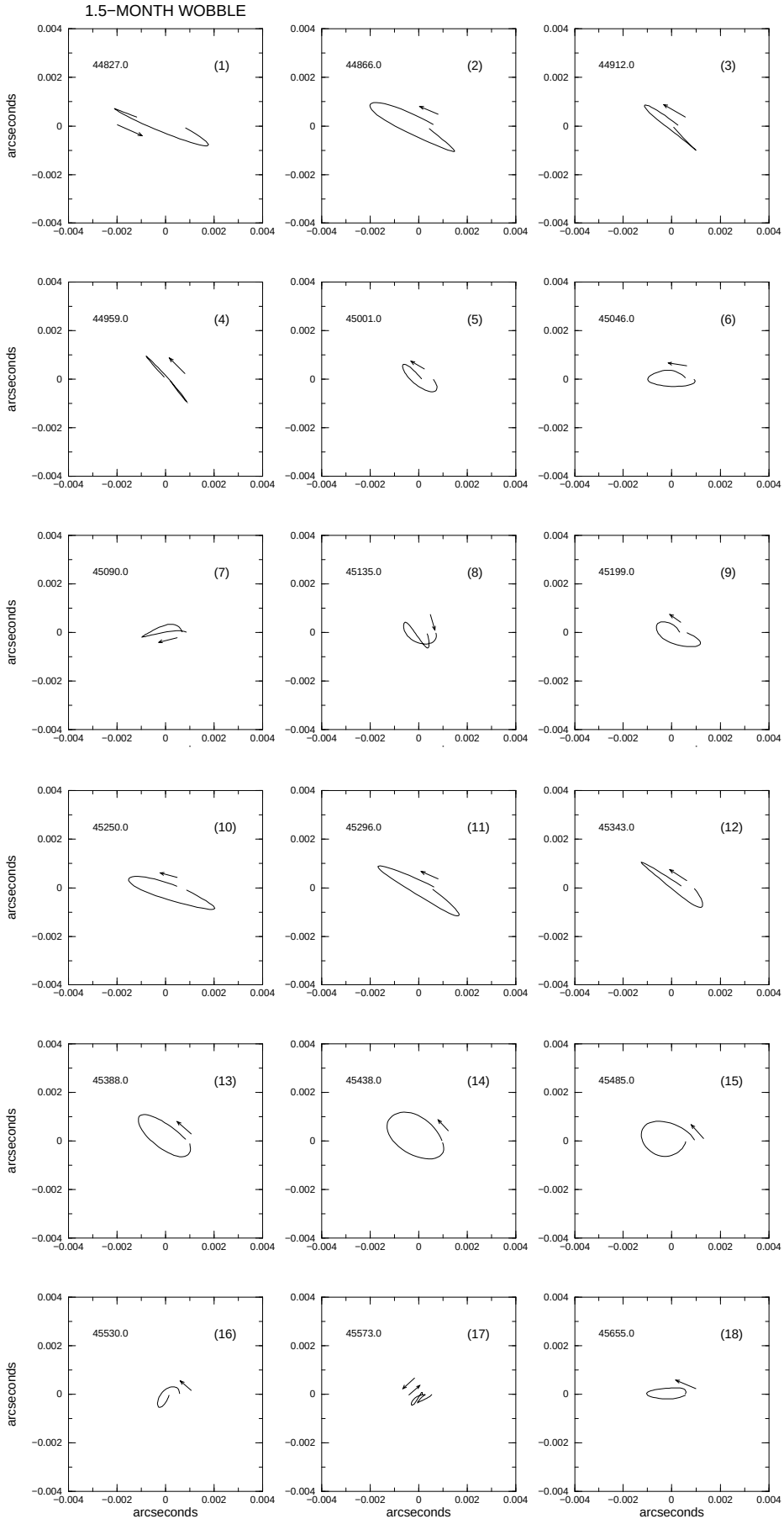

Figure A7. 1.5-month wobble. The curves shown are the revolution motions over the analysis interval (from left to right and from top to bottom). The x_1-axis points towards the Greenwich meridian, and the x_2-axis towards 90^oE longitude. For the revolution times in years, see Fig. 4

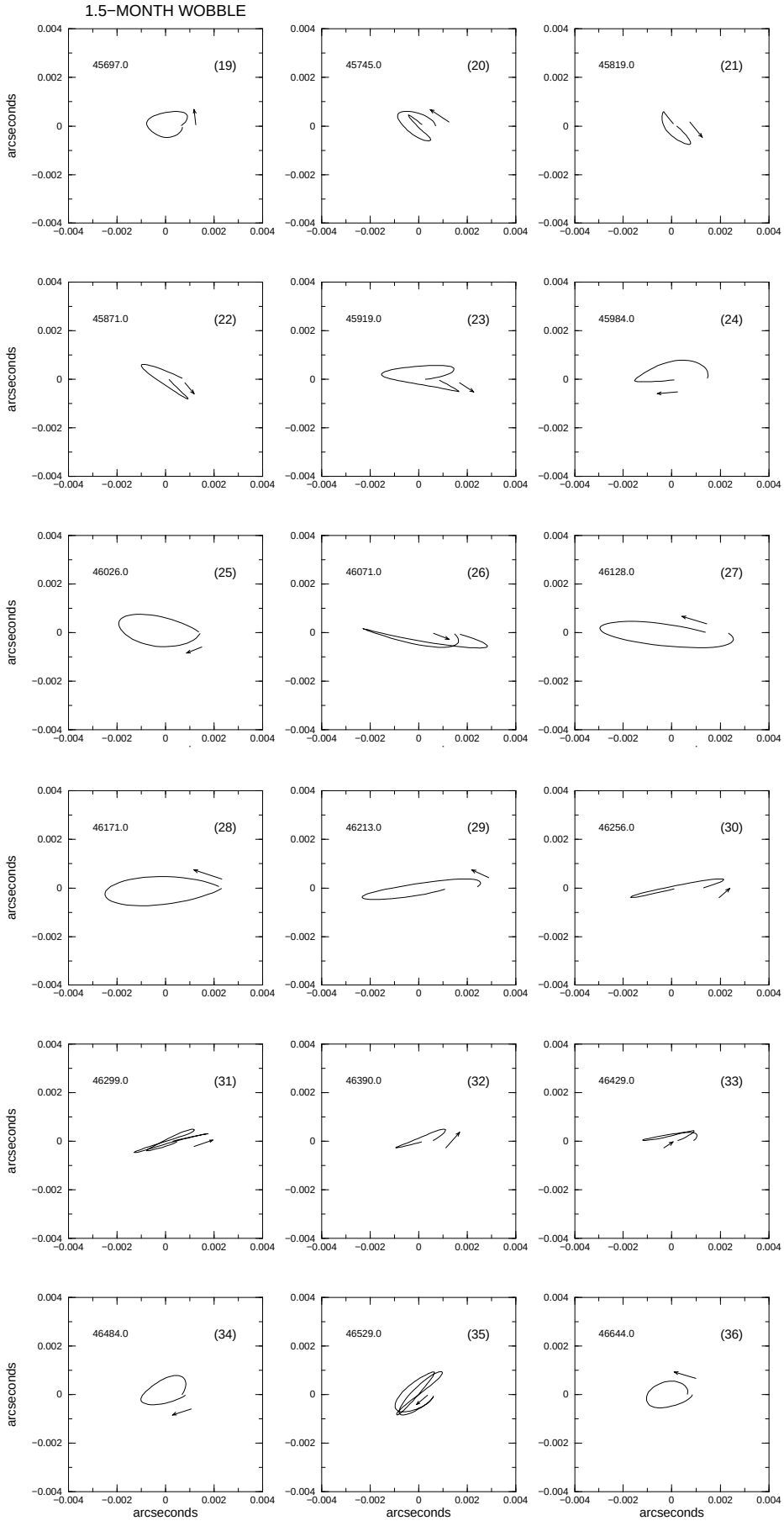

Figure A7. Continued

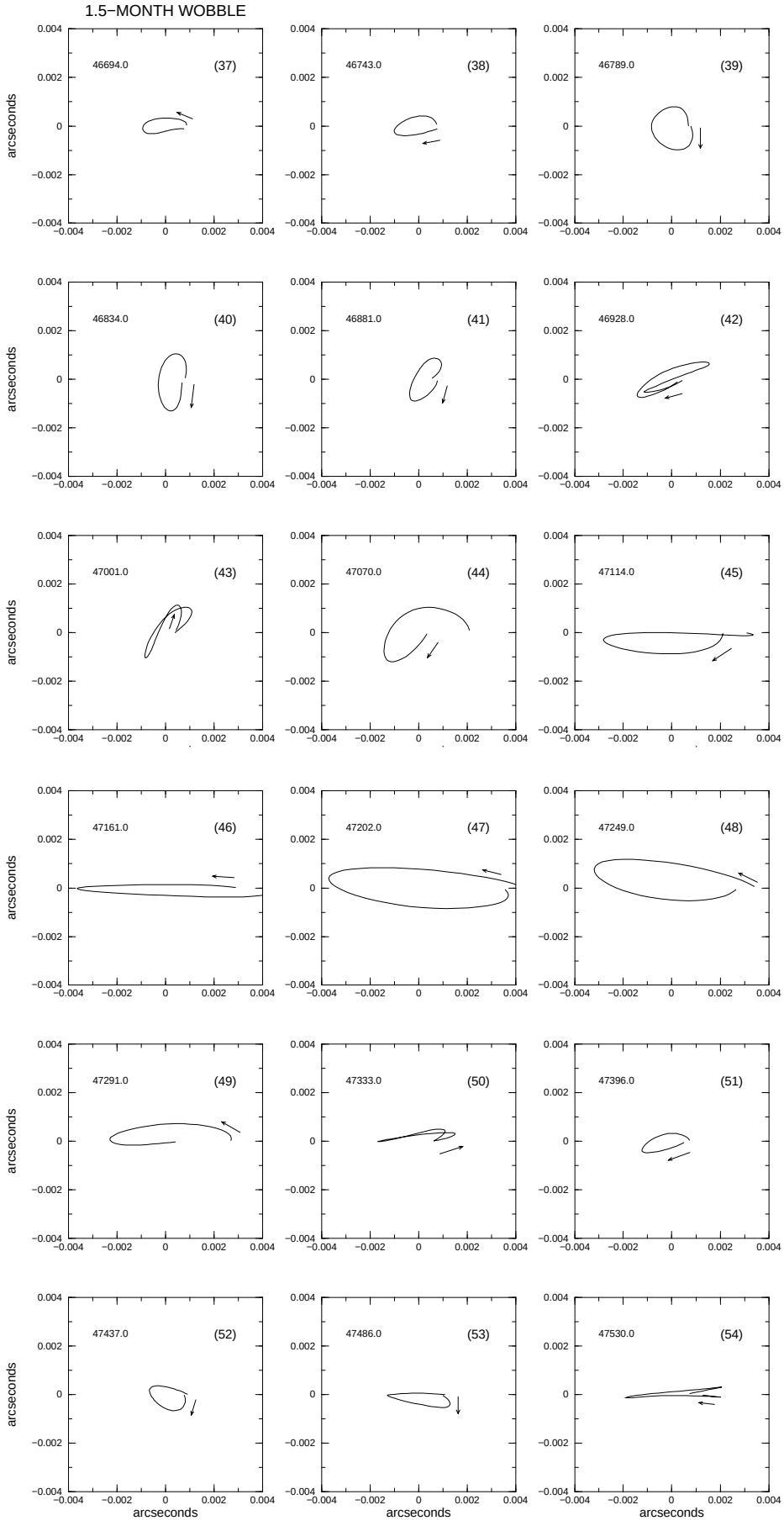

Figure A7. Continued

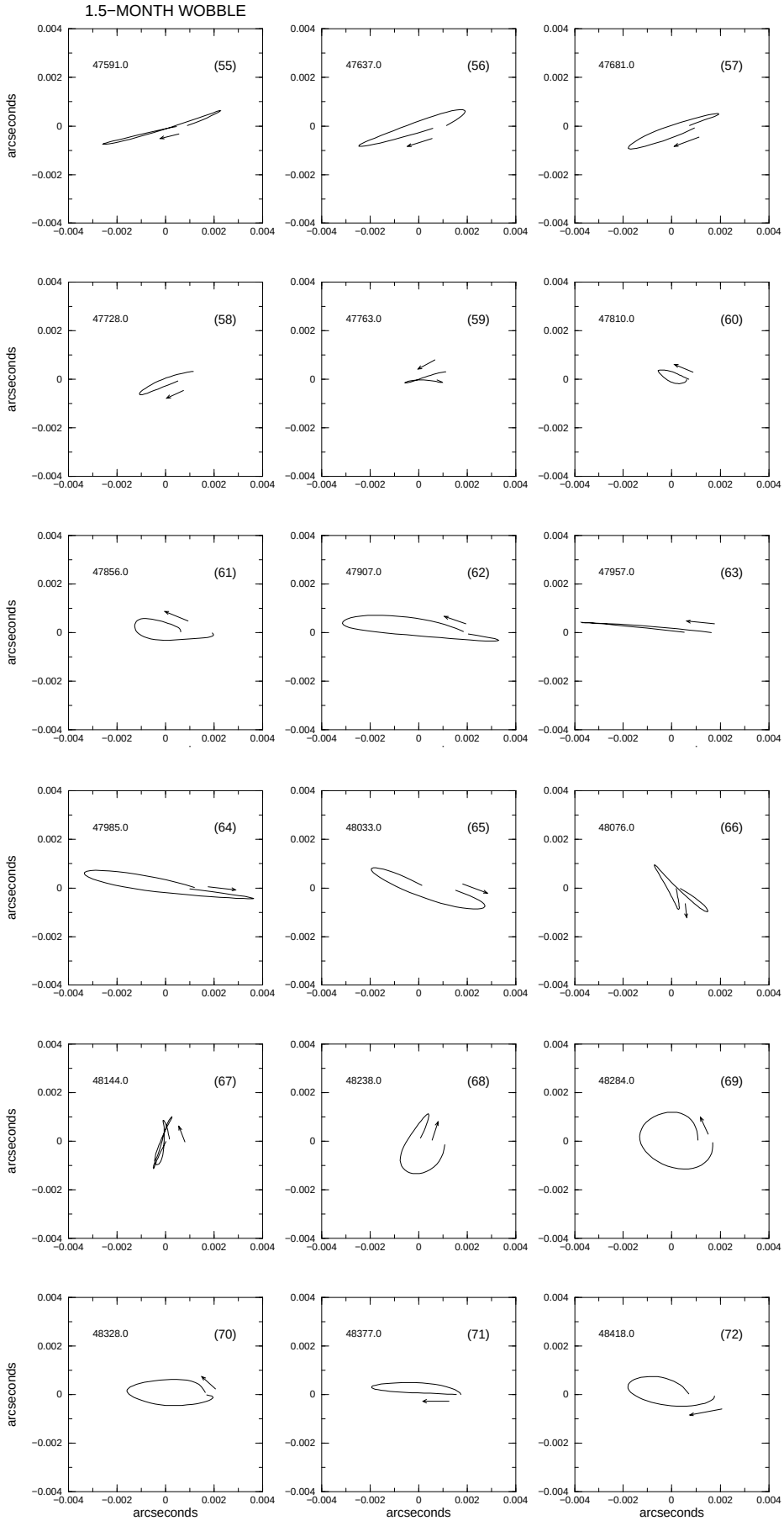

Figure A7. Continued

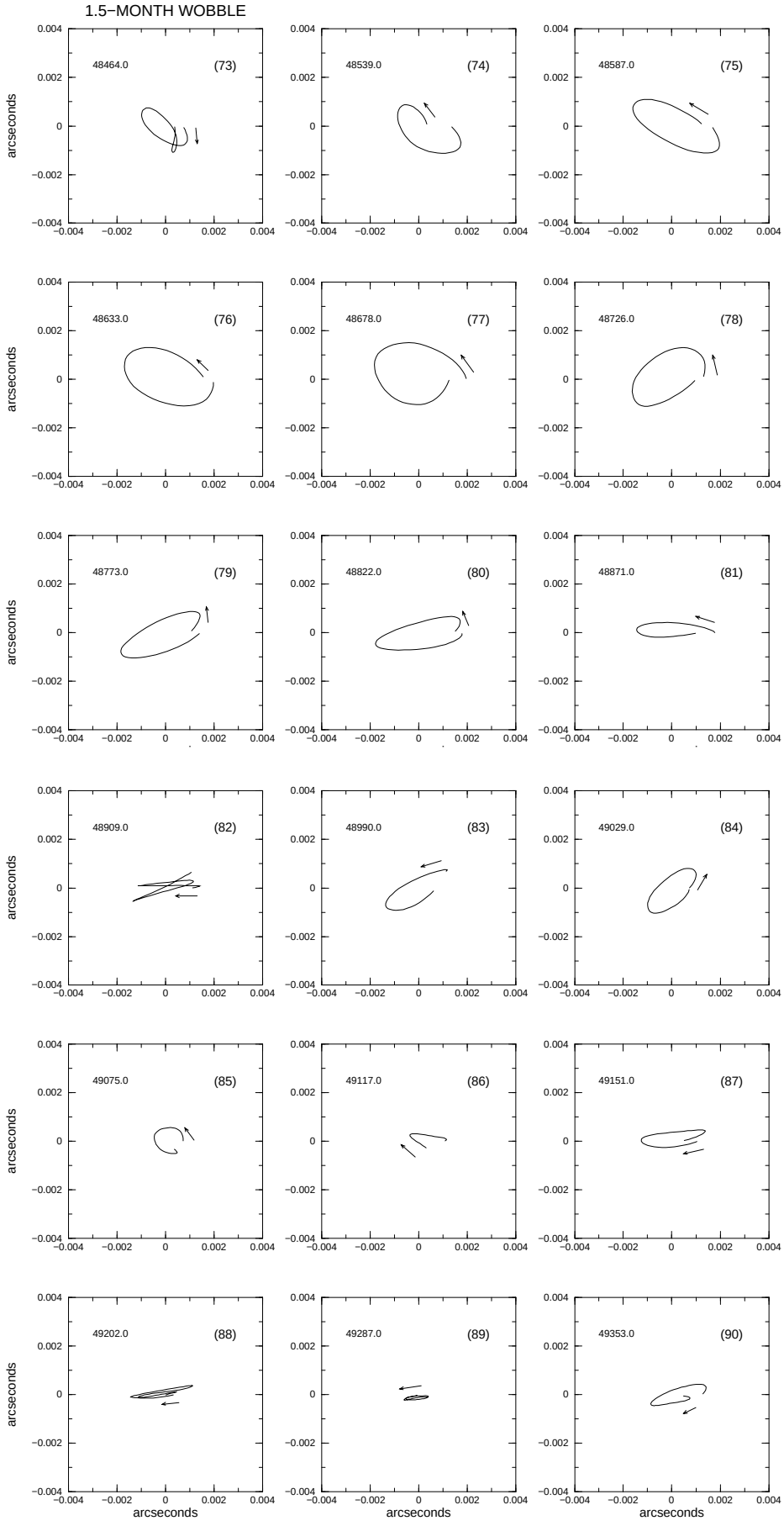

Figure A7. Continued

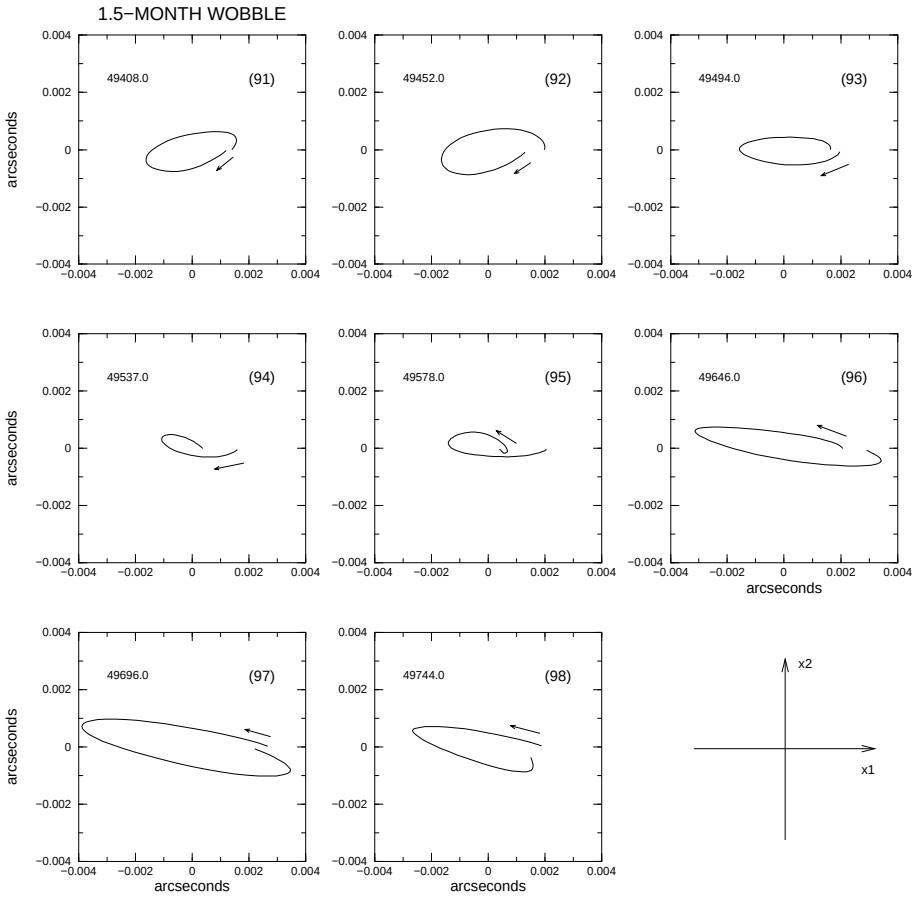

Figure A7. Continued

References

Chandler, S. C., 1891, 1892. On the variation of latitude. *Astron. J., 11 and 12*, Boston.
Dick, S., McCarthy, D. and Luzum, B. (eds.), 2000. *Polar motion: Historical and scientific problems*, ASP Conf. Ser. Vol. 208. 641 pp.
Euler, L., 1758. *Du Mouvement de Rotation des Corps Solides autour d'un Axe Variable*. Histoire de l'Académie Royale des Sciences et Belles Lettres. Berlin.
Fedorov, E. P., Korsun, A. A., Major, S. P., Panchenko, N. I., Taradi, V. K., Yatskiv, Ya. S., 1972. *Polar motion of the Earth from 1890.0 to 1969.0* (in Russian), Ukrainian Acad. Sc. Kiev.
Gross, R. S., 2000. *Combinations of Earth Orientation Measurements: SPACE99, COMB99, and POLE99*, JPL Publication 00-5, Pasadena, California.
Helmert, F. R. und Albrecht, Th., 1899. Der internationale Polhöhendienst. *Astron. Nachr., 148*, 3532, 4–56.
Höpfner, J., 1995. Periodische Anteile in der Erdrotation und dem atmosphärischen Drehimpuls und ihre Genauigkeiten, *ZfV*, *120*, 1, 8–16.
Höpfner, J., 1996. Polar motion at seasonal frequencies, *J. Geodynamics*, *22*, 1/2, 51–61.
Höpfner, J., 2000. The International Latitude Service - a historical review, from the beginning to its foundation in 1899 and the period until 1922, *Surveys in Geophysics*, *21*, 5/6, 521–566.
Höpfner, J., 2001a. Chandler and annual wobbles based on space-geodetic measurements. Paper presented at the XXVI General Assembly, EGS, Nice, France, 26-30 March 2001. *J. Geodesy* (in press).
Höpfner, J., 2001b. Polar motions with periods of the order of a half-Chandler period and less in their temporal variability. Paper presented at the XXVI General Assembly, EGS, Nice, France, 26-30 March 2001. *J. Geodesy* (in press).
IERS, 2000. *1999 IERS Annual Report*. Central Bureau of IERS. Observatoire de Paris.
Kołaczek, B., Kosek, W., Schuh, H., 2000. Short-period oscillations of Earth rotation. In: Dick, S., McCarthy, D. and Luzum, B. (eds.), *Polar motion: Historical and scientific problems*, ASP Conf. Ser. Vol. 208, 533–544.
Kosek, W., Nastula, J., Kołaczek, B., 1995. Variability of polar motion oscillations with periods from 20 to 150 days in 1979-1991, *Bull. Geodesique*, *69*, 308–319.
Kosek, W., Kołaczek, B., 1997. Semi-Chandler and semi-annual oscillations of polar motion, *Geophys. Res. Lett.*, *24*, 2235–2238.
Küstner, F., 1888. *Neue Methode zur Bestimmung der Aberrations-Constante nebst Untersuchungen über die Veränderlichkeit der Polhöhe*. Beobachtungs-Ergebnisse der Königlichen Sternwarte zu Berlin, Heft 3, Berlin.
Lagrange, J. L., 1788. *Mécanique Analitique*. Paris.
Peters, C. A. F., 1844. Resultate aus Beobachtungen des Polarsterns am Ertelschen Verticalkreise der Pulkowaer Sternwarte. *Astron. Nachr.*, *22*, Nr. 509–512. Altona.
Poinsot, L., 1834. Théorie Nouvelle de la Rotation des Corps. *L'Institut. Journal Général des Sociétés et Travaux Scientifiques*, *2*, Paris.